Lebanese American University

ELE 594: Undergraduate Research Project

A MODIFIED HYBRID MULTI-OBJECTIVE GA AND LSF ALGORITHM FOR OPTIMAL SITING AND SIZING OF PV-BASED DISTRIBUTED GENERATION IN DISTRIBUTION NETWORKS CONSIDERING DIFFERENT TYPES OF LOADS

Advisor: Dr. Raymond Ghajar

Preparation: Jessica Korkmaz - 201801005

Final Report

Fall 2022

Abstract

Many methodologies have been developed for the problem of optimal siting and sizing of photovoltaic (PV) distributed generation in distribution networks. However, clear solar potential assessment and variability of load constitutions at buses are aspects that are still missing in current optimization formulations. In this paper, a new methodology that uses the Multi-Objective Genetic Algorithm (MOGA) is proposed for the optimal allocation of PV-based distributed generation units (PV-DGs) in distribution networks. The method aims at minimizing active power losses, voltage deviations, and energy costs using a practical model that considers both the solar potential of each bus and variable load classifications. For this purpose, a modified MOGA algorithm that incorporates a Loss Sensitivity Factor (LSF) of solar potential in the optimal allocation problem at peak load is developed and compared to the traditional MOGA algorithm. The hybrid MOGA-LSF algorithm involves a two-step optimization problem. In the first step, the candidate buses for optimal allocation of PV DGs are specified using the LSF algorithm and in the second step, the radial power flow nested within the MOGA formulation is used to determine the sizes of the DGs to be installed. The time variations of loads are modeled by dividing a typical summer day into six intervals, each having different solar irradiance levels. Loads profiles of different classifications are also modeled for each candidate bus. The proposed technique is applied to the IEEE-15 bus radial distribution network to illustrate its effectiveness.

Table of contents

Table of figures

Table of tables

I. INTRODUCTION

The distribution network is the final stage of an electric power supply system where the power is distributed to customers. The main problem of distribution systems is the power losses created by the current flow (I^2R losses) which can account for 70 % of the total losses in the power system network. One of the solutions to decrease these losses is the connection of local power supply sources also known as distributed generation (DG) sources [2].

Distributed generators are small power units that can be either powered by renewable or nonrenewable sources and located near customer sites in distribution networks. Distributed power generation models that are mainly encountered in the literature can be divided into two types: Deterministic DG models and stochastic DG models. On the one hand, deterministic models mainly include DGs that can be dispatchable, which means that their power output can be controlled by increasing or decreasing the energy supply sources. Some common examples of deterministic DGs include gas turbines and fuel cells. On the other hand, stochastic DG models consider the intermittent and unpredictability of the supply sources. This is the case of renewable DGs such as wind energy and solar photovoltaic (PV) units that are characterized by a variable input supply of power that depends essentially on the local weather conditions [1].

Over the last decade, the installation of DGs has become more popular with the advancement in the use of renewable sources of energy [15]. Apart from reducing costs as the initial investment of building new power plants is replaced by smaller and distributed investments [1], the difficulties in building new transmission lines and the technological progress in small-scale power generation units [16], the integration of renewable energy resources (RESs) in distribution networks have increased rapidly with the growing interests to reduce the emission of greenhouse gases from fossil fuel sources and the growing environmental concerns of air pollution and global warming [1]. Among renewable resources, wind and solar photovoltaic (PV) sources are currently widely used as they are being designed for small-scale installations which makes them suitable to integrate into distribution systems [23]. This is why research has been primarily focusing on finding methods to make this integration more reliable and economically feasible. Furthermore, renewable DGs present lots of advantages in distribution networks such as minimization of power losses, improvement in voltage profiles, enhanced system reliability [1], peak shaving, and relieving overloaded distributed lines [13]. However, these benefits can only be observed if the renewable-based DGs are properly placed and sized. In fact, the main challenges of renewable resources lie in their intermittent nature which can be the cause of economic and technical issues for network operators. Hence, if the installation of these DGs is not well planned, undesirable effects might occur such as bidirectional power flow, stability issues, harmonic instability, and voltage fluctuations that can threaten the quality of the power delivered to consumers [11].

Consequently, regarding what was stated above, the problem of optimal allocation of DGs in distribution networks is of crucial importance and has been studied extensively in the literature.

The optimal DG placement problem consists of finding two parameters: the location of DGs in the network and their size or capacity that can theoretically vary from 0 to 100 % of the total demand that needs to be met [2].

II. Literature review

This literature review presents an overview of the research work that has been done on the optimal allocation of DGs in distribution networks. The literature will be divided based on the types of DGs that were to be allocated for each paper: References [3-4] focus on dispatchable DGs alone, references [5-10] examine wind-based DGs only, references [11-12] include both PV and wind-based DGs, references [13-16] consider both dispatchable and non-dispatchable DG types and the remaining research (references [17-27]) targets solar PV units only. For each type of DG being allocated, different types of optimization techniques are used. They can be classified into analytical techniques such as loss sensitivity factor (LSF) and the improved analytical method (IA), classical techniques including linear programming (LP) and mixed-integer nonlinear programming (MINLP), metaheuristic techniques such as genetic algorithm (GA), particle swarm optimization (PSO), Ant lion optimization (ALO), artificial bee colony optimization (ABC) and ant colony optimization (ACO), artificial intelligence techniques that integrate fuzzy decision-making tools and hybrid techniques which combine two analytical techniques, two metaheuristic techniques (for example GA-PSO) or analytic and metaheuristic techniques (LSF-ALO for instance). Since the integration of renewable sources in distribution networks is not an easy task as most of the allocation problems are formulated as MINLP problems, there is no guarantee that the optimal solution can be found using exact optimization techniques. This is why most of the literature has been relying on metaheuristic techniques through algorithms to solve problems of optimal sizing and allocation of PV DGs (PSO and GA being the most popular techniques for this purpose[13]). Even though metaheuristic techniques may trap the solution in a local minimum [4], these algorithms have lots of advantages in terms of adaptation to all types of problems and finding solutions in a wide search space without having to dive into the complexity of the problem [21].

1. Allocation of dispatchable DG units in distribution networks

The early works on the problem of optimal allocation of distributed generation considered only dispatchable DGs mainly fuel cells. For instance, the authors in [3] use a hybrid GA and OPF algorithm to determine the best sites to connect DGs and their respective capacities. The hybrid implementation is required because the GA used alone, will find the optimal locations but for predefined sizes, and the OPF alone would provide continuous capacities but at pre-specified locations. The single objective function considers the loss target where DNOs are rewarded if the losses are below a certain target and penalized if the losses are above this target. In [4], a hybrid analytical and metaheuristic optimization technique is proposed to optimally allocate DGs in the distribution network to reduce the network power losses: the candidate buses are chosen using

an extended LSF method and a fussy logic controller (FLC). The results obtained are then used as initial values to the sine-cosine algorithm (SCA) to specify the optimal sizes and locations. The paper also considers a new categorization of DGs. Effectively, it considers three types of DGs based on their ability to inject or consume reactive power. Both [3] and [4] show that the optimal allocation achieves huge decreases in power losses and an enhanced voltage profile. However, both works included deterministic DGs only and further showed the need to consider probabilistic energy sources under network constraints.

2. Allocation of wind-based DG units in distribution networks

With the increase in carbon-dioxide emissions and the growing concerns regarding global warming, wind energy became one of the most important types of renewable energies and a lot of European countries are currently working on increasing its penetration mainly in distribution networks. However, wind energy integration into the grid comes with challenges regarding voltage deviation and stability as well as power losses. This is why a proper allocation of DGs is of crucial importance to increase the benefits of integrating distributed generation into distribution networks on the operators [9]. Reference [5] models the uncertainty in the power supply by using a probabilistic-based planning technique to build all possible scenarios of operation of the distribution system. This model is then incorporated within an OPF formulation to compute the total energy losses. The authors showed that probabilistic planning achieves better results in terms of losses since the optimization considers all the possible combinations of load and supply and is a good representation of the actual network. Reference [6] considers the minimization of total expected active power losses of the system by controlling the wind turbines' power factor. The optimal power factor angles for wind turbines are determined from a stochastic optimization and the autocorrelation and cross-correlation of the wind power are modeled using the bivariate LARIMA model. The paper concludes that once the optimal power factor setting for wind power is determined, significant loss minimization can be achieved. In [7], the optimal allocation of wind turbines in distribution networks is carried out by combining multi-objective GA and the market based OPF to jointly minimize the total energy losses and maximize the net present value of wind turbines' investments. To evaluate both objective functions simultaneously, the nondominated sorting GA II (NSGA II) procedure is applied to find multiple Pareto-optimal solutions. The main results showed that the dispatched power of WTs increases proportionally to the increase in load demand. The authors in [8] propose a hybrid PSO and optimal power flow to maximize the net present value of the investment done on WT- based generations. Modeling of generation and load is also done based on the joint probability of occurrence of wind and demand to come up with several wind/demand scenarios and contingencies constraints are incorporated in the model. The outcomes revealed that the total dispatched active power of DGs decreases when contingency constraints are considered, and higher DG capacities are installed in locations that are close to the substation. A new optimization algorithm, the multi-objective artificial electric field algorithm (MOAEFA) was presented in [10] aiming to optimally allocate wind turbines in radial networks. The algorithm includes a fuzzy logic decision-making method to reduce power losses and minimize voltage deviations. The algorithm

is then compared to the PSO, GWO (grey wolf optimizer), and BSO (backtracking search optimization) search methods and the paper shows its superiority in achieving lower amounts of power loss and voltage deviation for both the single-objective and multi-objective placement of wind turbines.

3. Allocation of wind and PV-based DG units in distribution networks

Furthermore, the authors in [11] and [12] considered the allocation of both PV and wind-based DGs into distribution networks. In [11], a simple and flexible decision-making algorithm to optimally size and place renewable DGs of two types (wind and PV-based DGs) in distribution networks is suggested, and it is implemented on MATLAB and NEPLAN software. The optimal allocation is defined as the location and capacity of DG that will result in the smallest amount of power losses. The implemented algorithm achieved results comparable to those found by other methodologies in the literature. Moreover, [12] proposes a hybrid fuzzy logic controller (FLC) and ant lion optimization (ALO) algorithm to optimally allocate PV and wind-based DGs with different power factors. The problem assumes a multi-objective formulation where power losses, operational costs, voltage deviation index, and voltage stability index are all minimized. The technique achieves better power loss reduction and enhanced voltage profile as compared to the ALO-PSO and ALO methods in all three cases of unity, leading, and lagging pF for the DGs.

4. Allocation of dispatchable and non-dispatchable DG units in distribution networks

The following group of papers [13-16] considers that the diversification of types of DGs that are optimally placed may have various impacts on the stability and operation of the network. For instance, the authors in [13] focused on the simultaneous integration of both dispatchable (gas turbines) and non-dispatchable DGs (wind-based DGs) in distribution networks. The optimal location of wind and gas turbines DG units has been solved using the GA approach. The objective function is a cost function that includes annual DG capital costs, DG operation and maintenance costs, energy loss costs, and emission costs. The results showed that the DG allocation considering costs of emission resulted in better performance of the network than the case where the costs of emissions weren't considered. Similarly, in [14], the ant colony optimization (ACO) and artificial bee colony (ABC) optimization are combined to optimally allocate dispatchable and non-dispatchable DGs in distribution networks considering both load and wind uncertainties. ACO algorithm solves for optimal solutions and ABC makes sure that the ACO isn't trapped in a local optimum solution and converges to the global optimum solution. A probabilistic power flow based on the point estimate method (PEM) is also used to model the stochastic nature of both wind generation and load demand. The proposed hybrid technique achieved better loss reduction and better performance compared to PSO-CFA and ABC methods. Moreover, a new methodology based on the Water, energy, and food algorithm (WEFA) to determine the best size and location of DGs, was presented in [15] to minimize power losses that arise from a non-optimal placement of DG sources and emissions. The Dragonfly algorithm (DFA) was developed to solve for the best locations and sizes of the renewable DG sources and revealed noticeable improvements in both power losses and voltage profiles with low computation time. Reference [16] discussed the optimization of a distribution system that contains wind, PV, fuel cell, and

battery storage using PSO, to reduce the total costs of DGs, improve the voltage profile and decrease the usage of gas from the grid to reduce emissions, and this is done by considering different types of loads such as electrical, heating and cooling loads and their variation in time over a year. The observed results pointed toward improved voltage profiles following the optimal sizing and placement of DGs. Also, the installation of solar and wind-based DGs considerably decreased the amount of gas emitted.

5. Allocation of solar PV DG units in distribution networks

The optimal allocation of PV-based DG units was further discussed in [17-27]. As a matter of fact, for countries with high solar potential such as Lebanon, solar PV appears to be the most suitable technology as the PV generation output is strongly dependent on solar irradiation. Also, it doesn't require large areas of development such as wind energy [23]. Furthermore, research suggests that investments in building new distribution lines and feeders can be avoided if PV-based DG units are optimally placed and sized in regions of high concentration of load and can hence contribute to reducing the environmental impacts of fuel-based power generation. Nevertheless, the allocation of PV units into distribution networks displays some technical challenges mainly due to the intermittent nature of solar irradiance levels. So, to mitigate adverse effects such as rising voltages and reversal power flows, there is a need for analytical models to relate solar irradiance and PV injection into the network so that the integration of PV-based DGs happens as smoothly as possible [19].

The authors in [17] propose a clustering technique to optimally allocate PV DGs in distribution networks. To represent the fluctuating nature of the output power of PV modules and the variable nature of the load, the simulation must be run on the entire days of a full year hour by hour. As this approach is highly time-consuming and costly, the clustering technique finds the days that would be most representative of the yearly profile and run the simulation on these days only. The simulation is run over all seasonal levels of loads and for all clusters using the PSAT software. Then, the total power losses are calculated, and the best sizes and locations are deduced from the perspective of minimizing power losses. Furthermore, the authors in [18] consider the modeling of harmonics that were ignored in the literature under the assumption that the connection of DGs will affect total harmonic distortions (THDs) and individual harmonic distortions (IHD). The biography-based optimization (BBO) method is implemented to optimally allocate PVDGs to solve a multi-objective function that is composed of power loss reduction and voltage profile improvement while maintaining THD and IHD indices within their limits. The paper concluded that, although GA, PSO, and ABC can meet the harmonic constraints, their results are not as good as the BBO algorithm. In [19], a two-stage stochastic optimization model to optimally site and size PV DG units in distribution networks is implemented to minimize the costs incurred by the installation of PVs and the thermal loss they generate. Based on the allowed number of PV installations at each bus, the average panel area and inverter capacity of the PV DGs are determined. Moreover, a new optimization technique, the Modified Jaya Algorithm is presented in [20] aiming to find the optimal capacities and location of PV-based DG units under very high penetration levels. The algorithm indicated better performance than other existing methods in

minimizing power losses and improving the voltage profile in both low penetration levels and high penetration levels of PV DGs (around 300 %). In [21], the authors address the problem of minimization of losses by optimal placement and sizing of PV DGs units by using the MINLP model and the hybrid discrete-continuous modification of the vortex search algorithm (DCVSA) metaheuristic solution method. The paper considers 24 hours simulation where both demand and PV generation vary hour by hour and the analysis considers both the power losses in the peak hour and the overall losses over the full period considered. The DCVSA technique achieved a reduction in power losses that is 1.3% greater than the GAMS-BONMIN method.

As deduced from the above, the literature shows the need to find new optimization techniques with better numerical performance that can guarantee that the global optimum can be reached. Hence, [22] suggests a new hybrid algorithm: the modified arithmetic optimization algorithm (MAOA), that can be used to solve different MINLP problems. The objective function considers three types of costs: investment costs, energy purchase costs, and maintenance costs associated with PV units. The original AOA algorithm is enhanced by including a Gaussian distribution operator that can generate new candidate solutions. The results demonstrated that the implemented algorithm reaches the best optimal solution compared to the BONMIN in GAMS and metaheuristic techniques such as CBGA, NMA, and the original version of the AOA. Similarly, the authors in [23] develop a generalized normal distribution optimizer (DNDO) with a discrete-continuous codification to solve the problem of optimal PV allocation and sizing in the first stage. Then, in the second stage, the MINLP model is transformed into a simple power flow plow for distribution networks using the successive approximation power flow (SAPF) method. The objective of this optimal allocation is to reduce the investment and maintenance costs of the PV generators and the energy acquisition costs of the substation node.

Additionally, the genetic algorithm (GA) was extensively used for the problems of siting and sizing of PV-based DGs. Multi-objective GA has the advantage of simultaneously finding the Pareto-optimal solutions in a single run since it simultaneously searches for multiple solutions [7]. Therefore, the optimal placement and sizing of PV systems in distribution networks to minimize losses and improve the voltage profile is further discussed in [25] by using GA and Monte Carlo simulation to obtain the probability of irradiation and consumption in each hour of the day. The method considers the case where the solar potential is not the same at all buses of the network and can vary on four parts of the feeder from 0.95 to 1. Still the results showed that when the solar potential isn't the same in all the buses, the power losses are almost similar to the original scenario of equal solar potential at all buses. In [26], the real distribution network of the city of Kabul is studied and based on the GA optimization technique with the objective function of reducing power losses, the optimal placement and sizing of rooftop PV-based DG units is determined. The NR power flow is run over 24 hours to compute the fitness function. However, since only power losses are considered in a single objective problem, the results show that the optimal capacities of the PV DGs are very close to or equal to their maximum capacity. This shows that more constraints and objectives must be included to limit the integration of PVs and have more meaningful results. In [27], a two-step optimization approach is suggested to evaluate the

impacts of adding a battery energy storage system (BESS) into a distribution network that integrates renewable energy resources. In the first optimization step, the optimal size and location of the PV-based DG units are determined to achieve three objectives: minimization of active power losses, improvement of the voltage profile, and minimization of cost. In the second optimization step, the optimal size and placement of the BESS are determined to further reduce the objective functions. The problem is formulated as a multi-objective optimization and solved using the genetic algorithm technique and uses the time domain power flow to compute the fitness functions.

6. Gaps in the literature and the need for the study

Despite the work done on the optimal allocation of DG units in distribution networks, there is still a gap in the literature. Firstly, few works focus on the integration of both dispatchable and non-dispatchable DG into distribution networks [13]. This integration may have various impacts on the stability and operation of the network as highlighted in [14].

Secondly, most of the cited work [17-27] addressed the optimal allocation of PV DGs based on an optimization problem formulation. This problem is generally divided into two levels: the first level concerns the location of the DGs, and the second level concerns the problem of sizing. The first level is solved using sensitivity analyses or metaheuristic algorithms and the second level is solved by running several power flow simulations. However, as suggested in [24], it is not enough to only consider the optimization problem of allocation without performing a solar PV potential assessment at each bus. The locations that achieve the best objective functions may not have a high PV potential and vice versa. Hence, future work should consider both PV potential assessment (from geographic, economic, and technical perspectives) and the optimization algorithm integration simultaneously to solve the problem of optimal siting and sizing of PV DG units in distribution networks. It includes developing strategies for optimal allocation of PV DGs that also consider the feedback of the PV energy resource potentials alongside the power system's higher performance (classical optimization approach to reduce power losses and improve the voltage profile for example). This approach of assessing PV potential in different geographical locations will result in having more accurate DG limits and will save effort and time.

Thirdly, most of the cited literature assumed that there is a fixed type of load at each bus in a sense that the load could be considered fixed or variable and modeled stochastically as seen in references [5] and [6] for instance; however, none of the research considered the different types of customers at each bus such as industrial, commercial and residential consumers mainly. As a matter of fact, in [17] and [27], different types of loads were considered and residential, commercial, agricultural, and industrial customers were assigned randomly at buses. Nevertheless, each bus is modeled as having one type of load attached to it and the variability in the load constitution that is generally present in actual distribution networks is not considered. It is important to note that considering different types of loads may not lead to major differences in terms of power losses and voltage profile, but it will affect the allocation of PV units to buses and hence lead to different sizes and location values. Therefore, the development of more practical and closer to real distribution network models for both loads and DGs and new optimization problems that include both technical and economic objective functions, needs further attention.

Finally, as it was established by most research work that hybrid metaheuristic techniques may have higher chances of finding the optimal solutions [14] [24], new combinations of optimization techniques should be tried on the problem of optimal allocation of DGs in distribution networks to test their performance and explore their potential in finding better solutions than the existing techniques.

III. Problem formulation and system modeling

In this research, a new methodology for the optimal siting and sizing of PV-based distributed generation units (PV-DGs) in distribution networks will be developed. The method aims at minimizing active power losses, voltage deviations, and energy costs using a practical model that considers both the solar potential of each bus and variable load classifications. The multi-objective genetic algorithm (MOGA) and the radial power flow nested within this algorithm will be used to determine the sizes and locations of the PV DGs to be installed. The load profile of a typical summer day will be divided into six configurations and different load classifications will be considered. To show the importance of solar potential assessment at buses in the optimization problem, a modified hybrid MOGA-LSF algorithm will be proposed for the optimal allocation of PV DGs at peak load. It will also be compared to the traditional MOGA algorithm and the hybrid MOGA-LSF that do not incorporate any solar potential evaluation.

1. Objective functions

In this report, the optimal allocation of PV DGs is done based on three objective functions: total active power losses, voltage deviation, and total energy cost. Each of these objective functions along with its respective set of constraints will be explained in what follows.

A. Active power losses

The first important objective function to consider is the power losses in distribution lines that can be very high due to feeders being far away from load centers. The amount of power loss will depend on the location and size of the DGs because it varies with the squared magnitude of the traveling current and the resistance of the branch [15]. Therefore, minimization of power losses can be achieved by optimal placement and sizing of the DGs.

The distribution networks that are targeted in the proposed methodology may be radial or meshed even though the radial configuration is the most common one for distribution networks because of its simplicity and the fact that it achieves lower costs. In this configuration, the main feeder supply various areas or loads through a common radial line [2]. If the distribution system is radial, the power flow becomes easier to solve as the power summation or backward-forward sweep algorithms can be used instead of Newton's power flow. In the proposed methodology,

the system considered is radial. Hence, the power summation algorithm of the MATPOWER package is used to solve the power flow problem with less computation time.

To compute the total active power losses after the installation of the PV DGs at each bus, the PV-based DGs are treated as PQ nodes where both P and Q can be controlled independently. In the case of the PQ node, the PV-DG will act as a negative load as explained in [27] and the new load at each bus can be computed as follows:

$$P'_D(i) = P_D(i) - P_{PV-gen}(i) \quad (1)$$

Where $P_{PV-gen}(i)$ is the installed PV capacity at bus number i based on the number of PV panels that is allocated at this bus, and $P'_D(i)$ is the new active power demand at bus i.

Also, the PV DGs are modeled as supplying reactive power at a constant power factor of 0.9. Note that this model will be compared to the case where PV DGs are set at unity power factor later in the report, to investigate the benefits of DG power factor regulation in distribution networks. Therefore, the reactive power at each bus will be computed in a similar way to the active power using the following equation:

$$Q'_D(i) = Q_D(i) - P_{PV-gen}(i) * \tan(acos(0.9)) \quad (2)$$

Where $Q'_D(i)$ is the new reactive power demand at bus i.

The constraints for the power flow that will be considered are as follows:

1. For the safe operation of the power system, the magnitude of the voltage at each bus must lie within the lower and upper bounds of the bus voltage:

$$V_i^{min} \leq V_i \leq V_i^{max} \quad (3)$$

2. The thermal capacity, defined as the thermal capacity limit of each line or transformer in MVA [3], sets a limit on the maximum amount of power transfer in each line as follows:

$$S_t \leq S_t^{max} \quad (4)$$

3. The power flow balance equations are given by:

$$P_{grid} + P_{gen-PV} = P_D + P_{losses} \quad (5)$$

$$Q_{grid} + Q_{gen-PV} = Q_D + Q_{losses} \quad (6)$$

The first objective function can therefore be defined as:

$$\min P_{loss}(PV) \quad (7)$$

B. Voltage deviation index

Another important objective function to consider is the voltage deviation which is defined as the deviation in the bus voltages from the reference voltage of 1 per unit. These deviations occur due to the current flowing in the network lines and the voltage drop that will result [10]. Therefore, minimizing voltage deviations will contribute to an enhanced voltage profile. The objective function is formulated as defined in [27]:

$$\min VD_i = \sum_{i=1}^{n} |1 - V_i|^2 \quad (8)$$

Where n is the total number of buses.

C. Total energy cost

The third objective function is a cost function that is defined as:

$$Total\ cost = LCOE_{slack} * E_{slack} + LCOE_{PV} * E_{PV} \quad (9)$$

Where E_{slack} is the total energy generated by the slack and E_{PV} is the total energy generated by the PV DGs. Note that in the model, the total cost will be computed for each configuration. So, the energy will be computed for a one-hour interval at each iteration.

2. System modeling

A. Modeling of daily output of the PV system

To account for the intermittency of the solar PV resource, the model considers a typical day in September in Lebanon. The first 6 hours of the day (1 AM to 7 AM) constitute the first configuration. During this time interval, the hourly solar irradiance and the ambient temperature in Beirut are both recorded, and average solar irradiation and ambient temperature are computed for the entire configuration. Note that solar irradiance defines the amount of solar power that reaches the surface of the earth and is given in Watts per meter square of area. Depending on the location of the PV panel, the position of the earth relative to the sun, and the current climatic conditions, the solar irradiation amounts will vary on an hourly basis [1]. The second configuration will account for the next four hours of the day, from 8 AM to 12 PM, and the same procedure will be followed for the remaining configurations. All the configurations with the computed solar irradiance and ambient temperature are shown table 1 below:

Table 1: Solar irradiance and ambient temperature for the six configurations

Time t	Solar irradiation s (in kW/m^2)	Ambient temperature T_a	Configuration	Average irradiation	Average ambient temperature
1	0	26	Configuration 1	0.00843	25.57
2	0	26			
3	0	25			
4	0	25			
5	0	25			
6	0	26			
7	0.059	26			
8	0.266	28	Configuration 2	0.503	27.75
9	0.451	28			
10	0.601	27			
11	0.694	28			
12	0.76	28	Configuration 3	0.742	28
13	0.761	28			
14	0.705	28			
15	0.596	28	Configuration 4	0.33675	28
16	0.444	28			
17	0.257	28			
18	0.05	28			
19	0	27	Configuration 5	0	26.25
20	0	26			
21	0	26			
22	0	26			
23	0	26	Configuration 6	0	26
24	0	26			

As expected, configurations 1, 5, and 6 are characterized by a solar irradiance of zero since they are associated with the hours of the day characterized by the absence of the sun.

B. Solar PV output calculation for each configuration

The optimal allocation of PV DGs presented in this report consists of determining the number of PV panels to be placed at each bus. The type of PV panel considered for this analysis is the LG NEONR 365 W panel [29] whose electrical properties and temperature characteristics are summarized in the first column table 2 below:

Table 2: Electrical properties and temperature characteristics of the LG 365 W panel

Electrical Properties (STC *)

Module	365	360	355	350
Maximum Power (Pmax)	365	360	355	350
MPP Voltage (Vmpp)	36.7	36.5	36.3	36.1
MPP Current (Impp)	9.95	9.87	9.79	9.70
Open Circuit Voltage (Voc)	42.8	42.7	42.7	42.7
Short Circuit Current (Isc)	10.8	10.79	10.78	10.77
Module Efficiency	21.1	20.8	20.6	20.3
Operating Temperature	-40 ~ +90			
Maximum System Voltage	1000			
Maximum Series Fuse Rating	20			
Power Tolerance (%)	0 ~ +3			

Temperature Characteristics

NOCT	44 ± 3 °C
Pmpp	-0.30 %/°C
Voc	-0.24 %/°C
Isc	0.04 %/°C

Based on the above table , we define the following constants and their respective values:

$P_{DC,STC} = rated\ power\ of\ module\ under\ STC\ conditions = 365\ W$

$NOCT = nominal\ operating\ cell\ temperature = 44℃$

$P_{mpp} = percentage\ decrease\ in\ power\ for\ 1℃\ increase\ in\ temperature = 0.3\%$

$\eta_{mis} = efficiency\ after\ mismatched\ modules\ loss = 0.97$

$\eta_{dirt} = efficiency\ after\ dirt\ loss = 0.96$

$\eta_{inv} = inverter\ efficiency = 0.9$

$\eta = panel\ efficiency = 21\%$

The procedure to compute the AC power of each module is as follows:

We define $s_i = average\ solar\ irradiation\ in\ configuration\ i$

$Ta_i = average\ ambient\ temperature\ in\ configuration\ i\ in\ ℃$

Step 1: Temperature adjustment

We define $T_{cell} = Cell\ temperature\ at\ average\ ambient\ temperature\ Ta_i$

$$T_{cell} = Ta_i + \frac{NOCT - 20}{0.8} * 1 \qquad (10)$$

Which is the cell temperature when exposed to the ambient temperature Ta_i at 1-sun insolation (s=1 kW/m^2).

Step 2: Insolation adjustment

We define $P_{DC,PTC} = DC\ power\ of\ the\ PV\ panel\ under\ PTC\ conditions$

$$P_{DC,PTC} = P_{DC,STC} * \frac{s_i}{1} * \left[1 - \frac{P_{mpp}}{100}(T_{cell} - 25)\right] \qquad (11)$$

Step 3: Derating from DC to AC

We define $P_{AC,PTC} = AC\ power\ of\ the\ PV\ panel\ under\ PTC\ conditions$

$$P_{AC,PTC} = P_{DC,PTC} * \eta_{mis} * \eta_{dirt} * \eta_{inv} \qquad (12)$$

This is the AC power that is provided by a PV panel rated at 365 W and will depend on both the solar irradiance and the ambient temperature in which the PV panel is placed. Based on these equations, the AC power delivered by each PV module in kW can be computed for each configuration.

C. Maximum solar PV capacity at each bus

Each bus is characterized by the area available for installing PV panels in meter squares. From this area, the maximum PV capacity that can be allocated at each bus in kW, defined by the variable PV_{max} , can be computed based on the following formula:

$$PV_{max} = 1\left[\frac{kW}{m^2}\right] * Area\ [m^2] * \eta \qquad (13)$$

Table 3 below shows the area available for PV placement for each bus as well as the computed maximum PV capacity:

Table 3: Area available and maximum PV capacity for each bus in kW

Bus number	Area available (in m^2)	PV-max capacity (kW)
2	200	42
3	150	31.5
4	150	31.5
5	200	42
6	100	21
7	300	63
8	150	31.5
9	100	21
10	200	42
11	300	63
12	200	42
13	100	21
14	100	21
15	200	42

3. IEEE 15-bus test feeder

The IEEE 15-bus distribution system is shown in figure 1 below:

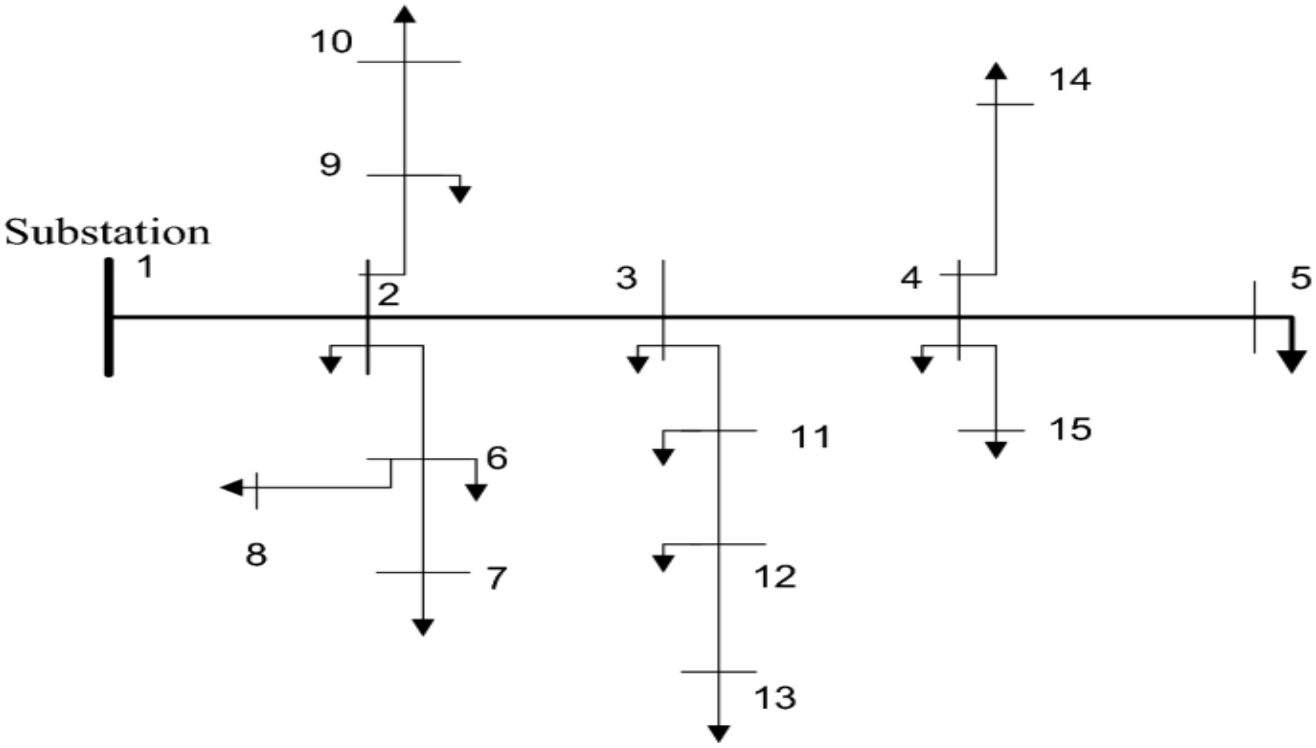

Figure 1: Single-line diagram for IEEE 15-bus distribution network

This test feeder is small and makes it appropriate to test the methodology presented here. The transmission parameters of the network are summarized in the following table [30]:

Table 4: Branch and load data for the IEEE 15-bus distribution network

Branch Number	Send Bus	End Bus	Resistance (Ω)	Reactance (Ω)	P (kW)	Q (kVar)
1	1	2	1.35309	1.32349	44.10	44.991
2	2	3	1.17024	1.14464	70.00	71.414
3	3	4	0.84111	0.82271	140.0	142.82
4	4	5	1.52348	1.02760	44.10	44.991
5	2	6	2.55727	1.72490	140.0	142.82
6	6	7	1.08820	0.73400	140.0	142.82
7	6	8	1.25143	0.84410	70.00	71.414
8	2	9	2.01317	1.35790	70.00	71.414
9	9	10	1.68671	1.13770	44.10	44.991
10	3	11	1.79553	1.21100	140.0	142.82
11	11	12	2.44845	1.65150	70.00	71.414
12	12	13	2.01317	1.35790	44.10	44.991
13	4	14	2.23081	1.50470	70.00	71.414
14	4	15	1.19702	0.80740	140.0	142.82

The active power demand in kW will be used in the model to represent the peak power load. However, for the reactive power Q, due to the sectoral and temporal divisions imposed in the

model, the reactive power values will differ at peak configuration 4 and hence in all other configurations.

4. Load modeling

To diversify the load profile, three load categories are considered: residential loads, commercial loads, and industrial loads. However, unlike most of the previous literature which considered each bus to have one type of load attached to it such as in [17] and [27], each bus will be composed of portions of different load categories as can be seen in table 5 below:

Table 5: Customer distribution by classification as installed at each bus

Bus #	Load distribution at peak (kW)	Customer distribution by classification as installed at each bus		
		Residential	Commercial	Industrial
2	44.1	70%	30%	0%
3	70	0%	0%	100%
4	140	50%	50%	0%
5	44.1	50%	50%	0%
6	140	50%	10%	40%
7	140	20%	70%	10%
8	70	100%	0%	0%
9	70	100%	0%	0%
10	44.1	50%	50%	0%
11	140	0%	0%	100%
12	70	75%	25%	0%
13	44.1	80%	20%	0%
14	70	0%	100%	0%
15	140	100%	0%	0%
Total	1226.4			

For example, 70 % of the load at bus 2 consists of industrial customers, and the remaining 30 % of it corresponds to commercial customers whereas bus 3 is a pure industrial load. In this way, the variability in the load constitution which is generally the case in buses of distribution networks is modeled.

In addition to the customer distribution classification installed at each bus, the time variations of the load during the day are also considered. In each configuration (C1 to C6) corresponding to the different time intervals of the day, the load will be distributed differently between residential, industrial, and commercial customers. For example, at night, commercial customers are very low whereas industrial customers tend to have a constant demand throughout the day. The graph below shows the load distribution according to the type of loads available during different periods of the day:

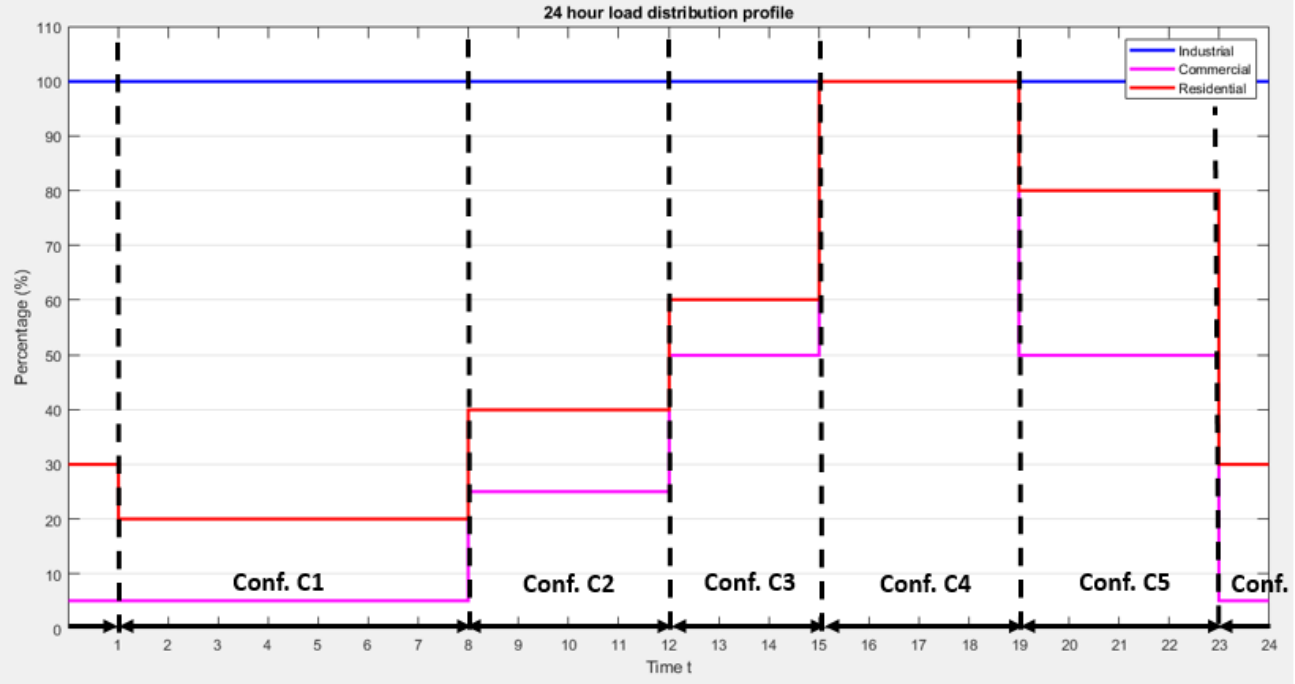

Figure 2: Daily load profiles of residential, commercial and industrial customers

Based on the daily peak load variation curves of the residential, consumer, and industrial sectors, industrial customers have a relatively flat load (a load factor of almost 1), while commercial and residential customers have a much lower load factor. Commercial customers have their peak early afternoon while residential customers have it in the later afternoon/early evening. For example, from 12 PM to 3 PM (configuration 3), residential customers are at 60% of their maximum demand and commercial customers are at 50% of their maximum demand. Note that in interval C4, the peak load of the system is achieved when all customer classifications have their peaks.

At this point, both spatial and temporal load distributions are modeled: the customer distribution by classification (industrial, commercial or residential) as installed at each bus (table 3) and the temporal load distribution by classification for different time intervals of the day (fig. 2). Both parameters are then convoluted to compute the active power demand at each bus for the corresponding configuration. To evaluate the reactive power demand at each bus, a fixed power factor was chosen for each type of customer as follows:

1. 0.9 PF lagging for industrial loads to comply with the requirements of the utility. Since industrial loads are highly inductive with PF between 0.7 and 0.8 lagging, they use PF correction to avoid paying penalties for high reactive power demand. The problem at hand focuses on small industrial loads because large industrial loads must maintain their power factor around 0.99 else a huge amount for penalty will have to be paid.

2. 0.85 PF lagging for residential loads to reflect the resistive nature of these loads. In fact, as opposed to industrial loads that are composed of rotating machines, residential loads are less inductive.
3. 0.8 PF lagging for commercial loads to reflect the air conditioning and heating loads of these loads. Usually, commercial loads are relatively small as compared to industrial loads and they are not subject to reactive power penalty by the electric utility.

The table below shows how the active power is obtained in period C1:

Table 6: Computation of the total load demand of each bus in period C1

Bus #	Load distribution at peak	Customer distribution by classification as installed at each bus				Load distribution by classification			Load distribution by classification at each bus			
						20.0%	5.0%	100.0%				
		Res	Com	Ind		Res	Com	Ind	Res	Com	Ind	Total demand in kW
2	**44.1**	70%	30%	0%		14.0%	1.5%	0.0%	6.17	0.66	0.00	**6.84**
3	**70**	0%	0%	100%		0.0%	0.0%	100.0%	0.00	0.00	70.00	**70.00**
4	**140**	50%	50%	0%		10.0%	2.5%	0.0%	14.00	3.50	0.00	**17.50**
5	**44.1**	50%	50%	0%		10.0%	2.5%	0.0%	4.41	1.10	0.00	**5.51**
6	**140**	50%	10%	40%		10.0%	0.5%	40.0%	14.00	0.70	56.00	**70.70**
7	**140**	20%	70%	10%		4.0%	3.5%	10.0%	5.60	4.90	14.00	**24.50**
8	**70**	100%	0%	0%		20.0%	0.0%	0.0%	14.00	0.00	0.00	**14.00**
9	**70**	100%	0%	0%		20.0%	0.0%	0.0%	14.00	0.00	0.00	**14.00**
10	**44.1**	50%	50%	0%		10.0%	2.5%	0.0%	4.41	1.10	0.00	**5.51**
11	**140**	0%	0%	100%		0.0%	0.0%	100.0%	0.00	0.00	140.00	**140.00**
12	**70**	75%	25%	0%		15.0%	1.3%	0.0%	10.50	0.88	0.00	**11.38**
13	**44.1**	80%	20%	0%		16.0%	1.0%	0.0%	7.06	0.44	0.00	**7.50**
14	**70**	0%	100%	0%		0.0%	5.0%	0.0%	0.00	3.50	0.00	**3.50**
15	**140**	100%	0%	0%		20.0%	0.0%	0.0%	28.00	0.00	0.00	**28.00**

The same procedure will be followed for the other periods and the load profile for 24 hours can be deduced in the table below where P_d and Q_d represent the active and reactive power demand in kW and kVAR respectively.

Table 7: Calculated active and reactive power of each bus for all six configurations of the model

Bus	Customer distribution	Conf. 1		Conf. 2		Conf. 3		Conf. 4		Conf. 5		Conf. 6	
		Pd	Qd	Pd	Qd	Pd	Qd	Pd	Qd	Pd	Qd	Pd	Qd
1	Slack =Feeder	-	-	-	-	-	-	-	-	-	-	-	-
2	70 % RES 30% COM	6.84	4.32	15.66	10.13	25.14	16.44	44.1	29.05	31.31	20.27	9.92	6.24
3	100% IND	70.00	33.90	70.00	33.90	70.00	33.90	70.0	33.90	70.00	33.90	70.00	33.90
4	50 % RES 50% COM	17.50	11.30	45.50	30.48	77.00	52.28	140.0	95.88	91.00	60.96	24.50	15.64
5	50 % RES 50% COM	5.51	3.56	14.33	9.60	24.26	16.47	44.1	30.20	28.67	19.20	7.72	4.93
6	50 % RES 10% COM 40% IND	70.70	36.32	87.50	47.10	105.0	58.40	140.0	81.00	119.0	67.08	77.70	40.66
7	20 % RES 70% C0M 10% IND	24.50	13.93	49.70	32.10	79.80	53.94	140.0	97.63	85.40	57.41	27.30	15.66
8	100 % RES	14.00	8.68	28.00	17.35	42.00	26.03	70.0	43.38	56.00	34.71	21.00	13.01
9	100 % RES	14.00	8.68	28.00	17.35	42.00	26.03	70.0	43.38	56.00	34.71	21.00	13.01
10	50 % RES 50% COM	5.51	3.56	14.33	9.60	24.26	16.47	44.1	30.20	28.67	19.20	7.72	4.93
11	100% IND	140.0	67.81	140.0	67.81	140.0	67.81	140	67.81	140.0	67.81	140.0	67.81
12	75% RES 25% COM	11.38	7.16	25.38	16.30	40.25	26.08	70	45.66	50.75	32.59	16.63	10.42
13	80 % RES 20% COM	7.50	4.70	16.32	10.40	25.58	16.43	44.1	28.48	32.63	20.80	11.03	6.89
14	100% COM	3.50	2.63	17.50	13.13	35.00	26.25	70	52.50	35.00	26.25	3.50	2.63
15	100% RES	28.00	17.35	56.00	34.71	84.00	52.06	140	86.76	112.0	69.41	42.00	26.03
Total	50 % RES 27% COM 23% IND	**418.93**	**223.9**	**608.21**	**349.95**	**814.28**	**488.58**	**1226.4**	**765.86**	**936.43**	**564.29**	**480.01**	**261.75**

5. Optimization

The optimization problem will be solved using the multi-objective genetic algorithm (MOGA) for all configurations. Furthermore, a hybrid MOGA-LSF algorithm and a modified MOGA-LSF algorithm will be also implemented on the peak load configuration C4. In what follows, each of these algorithms will be explained and the optimization constraints will be specified.

A. MOGA algorithm

The genetic algorithm (GA) is a metaheuristic search method inspired by the evolutionary theory of the origin of species. In nature, weak and unfit individuals are eliminated by the process of natural selection. The strongest ones possess the genes that will allow them to reproduce and pass these genes to future generations. As the individuals reproduce, genes might change through mutations and unsuccessful changes are again eliminated through natural selection. The solution vector x of the genetic algorithm is called a chromosome. The GA will operate with several chromosomes which form a population that is randomly initialized. As the search process advances, the population will start to include fitter individuals and will eventually converge to a single optimal solution. The GA uses two processes to generate new solutions: crossover and mutation. For the crossover, both parents are combined to form new individuals called offspring, that are expected to inherit the strongest features of their respective parents. By applying the crossover on several generations, the good genes are expected to remain and converge to the best solution. The mutation process is applied at the gene level. The mutation rate will be defined at the start of the genetic algorithm and is generally small so that new genes keep their resemblance to the original ones. In this way, the genetic diversity of the genes can be preserved. After those two operations are performed, a selection process is conducted to select the fittest chromosomes for the next generation based on their fitness value. Some selection processes include selection, ranking, tournament, and roulette wheel selection [31].

The genetic algorithm formulation makes it suitable to solve multi-objective problems where several objective functions are expected to be solved in a single run. Effectively, finding the optimum solution based on a single objective function will result in unacceptable results for the other objective functions because objective functions have generally conflicting goals. This is why finding a single solution that is best suited for all the objectives is almost impossible to find. For this purpose, two approaches are generally possible: the weight sum approach and the Pareto set approach. For the first approach, a weight is attributed to each objective function based on its relevance in the problem formulation. However, the problem with this approach is that it may be difficult to accurately find the weights of the objectives [31], and research found that the weight coefficient method may not be able to reach the optimal global solution of the objective function very well [10]. The second approach consists of finding the set of Pareto optimal solutions. These solutions are nondominated with respect to each other, meaning that while moving from one solution to another, improving one of the objective functions will lead to the worsening of at least one of the other objectives. Therefore, instead of having single solutions,

the decision-maker can choose the best solutions based on a trade-off. The multi-objective GA searches different regions of a solution simultaneously to find a diverse set of solutions without having to define scales or weight factors. It is one of the most popular heuristic search methods to solve optimization problems and is known for its robustness [31]. This is why for the implemented methodology, the MOGA will be used to determine the Pareto set of optimal solutions. The optimization process will aim to find the best location and capacity of the PV DGs to be allocated in the distribution network at hand. Hence, for this methodology, the output of the optimization process will be a set of Pareto optimal solutions. Each solution will be a vector called X represented as:

$$X = [x(1)\ x(2)\ x(3)\ \dots x(i)] \qquad (14)$$

Where $x(i)$ is an integer that represent the number of panels to be installed at bus number i. So, X will be a vector containing 15 variables since the system is formed of 15 buses. All the panels have the same rated power of 365 W, but they will provide a different output based on the amount of solar insolation available. The optimization is performed in two steps. In the first step, the optimal vector X is found for each of the six configurations found earlier. Then, in a second step, the solution vector X obtained for each configuration, is tested on every other configuration to determine the final optimal solution.

The problem formulation will require to set the following equality and inequality constraints:

$$x(1) = 0 \qquad (15)$$

$$\left\lfloor \frac{0.3 * PV_{max}}{P_{AC,PTC}} \right\rfloor \leq x(i) \leq \left\lfloor \frac{PV_{max}}{P_{AC,PTC}} \right\rfloor \qquad (16)$$

$$\left(\sum_{i=1}^{n} x(i)\right) * P_{AC,PTC} \leq 0.3 * \sum_{i=1}^{n} P_D(i) \quad (17)$$

For the constraint of equation 16, every variable $x(i)$ has a lower bound defined as 30 % of the maximum PV capacity that can be installed at each bus (table) divided by the power delivered by every panel considering both the insolation and ambient temperature adjustment as discussed in section III. 2 B. The upper bound will be the maximum PV capacity that can be installed at each bus divided by the power that can be delivered by each panel. Since $x(i)$ is an integer, a truncation to the nearest smaller integer is required. Note that the lower bound of 30% of the maximum PV capacity is chosen to avoid having very small PV capacities installed at certain buses. The last constraint (eq. 17) is related to the penetration of PV-based DGs in distribution networks. PV penetration is the quantity of PV power that can be injected into the feeder. It is calculated as the ratio of maximum PV power to the maximum apparent power of the load. However, high PV penetration levels can have negative effects on power quality mainly by increasing voltage fluctuations[20]. This is why the total amount of DG capacity that can be

installed must be limited to a certain percentage of the peak load in order not to violate system stability. Research on system stability has shown that the maximum penetration level of distributive generation, without violating the transient stability limit is 40 % of the total connected load [28]. So, for the current optimization problem, a maximum penetration level of 30% was chosen.

The flowchart below explains the proposed optimization process:

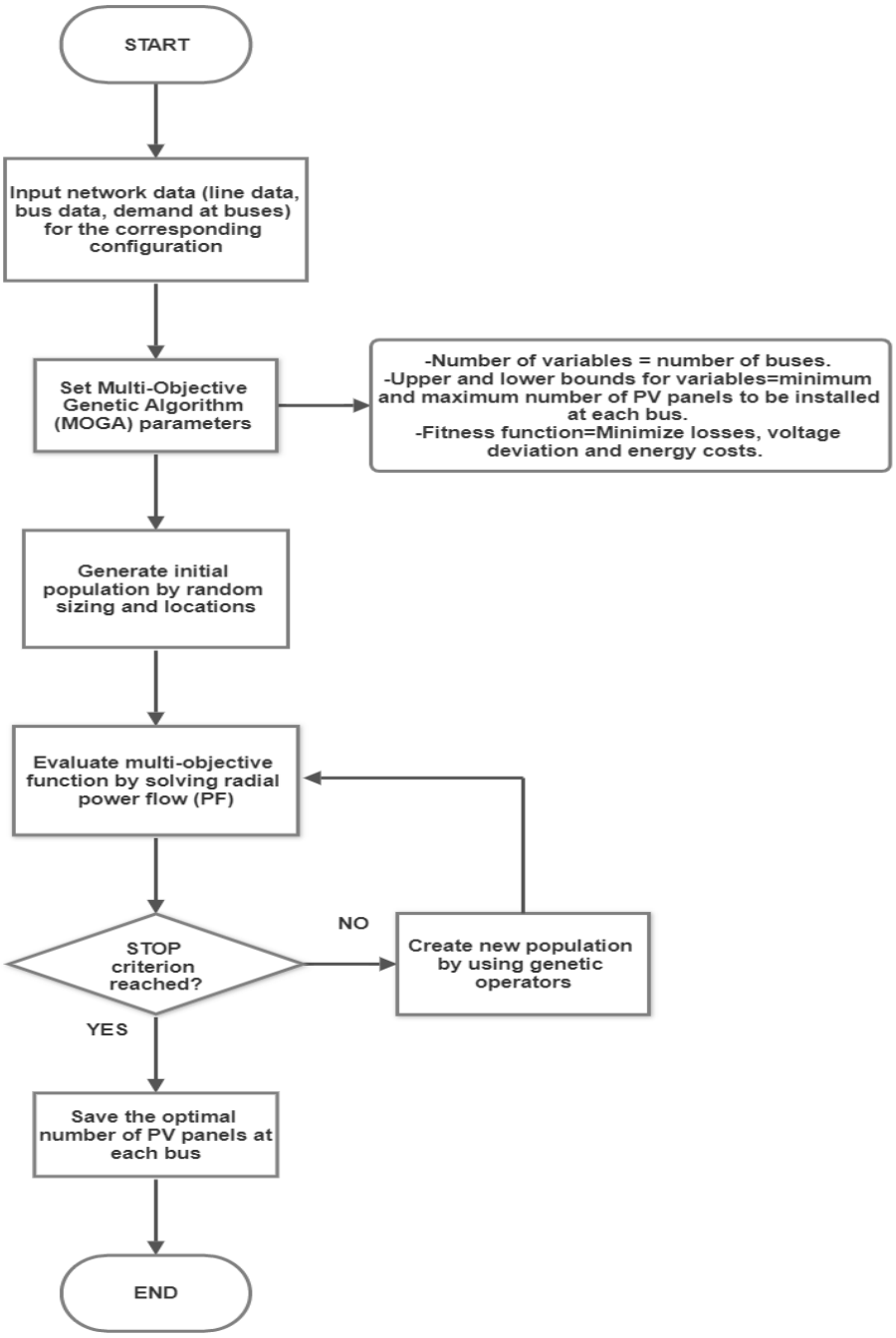

Figure 3: MOGA optimization methodology

First, the network data for the corresponding configuration is entered and the parameters of the MOGA are set including the constraints on the variables mentioned earlier. For each iteration, the power flow nested within the MOGA is used to compute the three objective functions for each individual within the population. The values of the fitness functions are then fed back into the MOGA which will continue the search process. The loop will continue until one of the stopping criteria is met and convergence is achieved. A set of Pareto optimal solutions will be obtained. As mentioned earlier, this process will be repeated for configurations C2, C3, and C4 (since there is no optimization in the other configurations as the solar irradiance is close to zero) to obtain the optimal solution for each of these configurations. Then, the optimal solution of each configuration is run on the other configurations to determine the best solution. The flowchart below shows the steps of the algorithm for configuration C2:

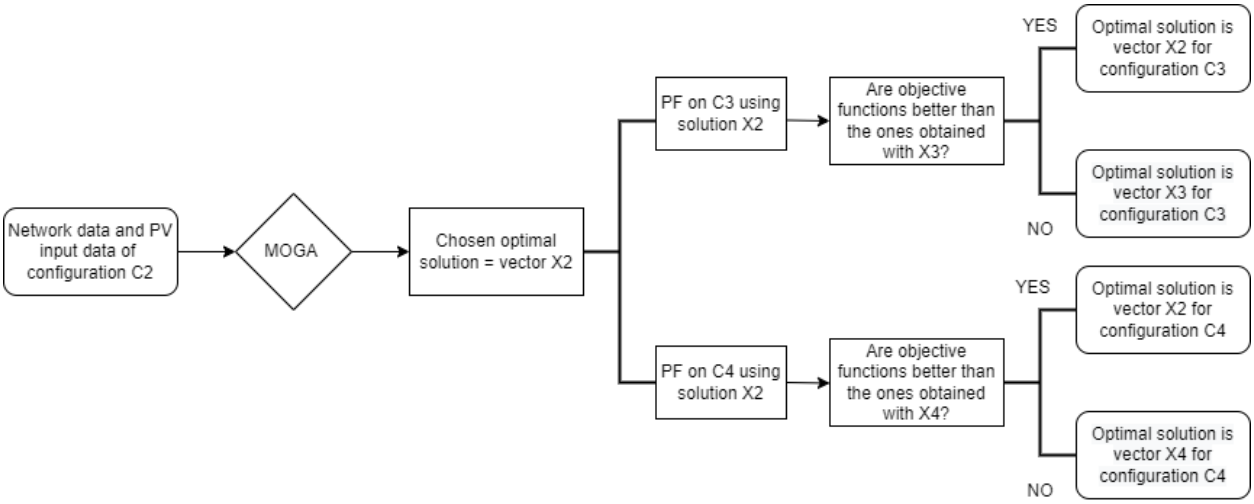

Figure 4: Optimization process applied on configuration C2

B. Hybrid MOGA-LSF algorithm

Hybrid optimization methods combine two algorithms that can be from the same type (ex: two heuristic techniques) or different types (classical and heuristic techniques). Hybrid optimization techniques make use of the strength of two optimization algorithms to come up with better results. Recent literature pointed out that combined hybrid methods may have higher probabilities of finding the optimal solution [4]. Here, the MOGA algorithm is combined with the LSF technique to solve the problem of optimal allocation of PV DGs in distribution networks. Note that to our knowledge, no research has combined these two algorithms for the problem of optimal allocation of PV-based DGs.

Considering a number r of DGs that are to be located in an n-bus distribution network, the number of possible combinations of DGs will be equal to C_r^n. Hence, even for a small distribution network, considering all possible combinations of locations is a demanding process mainly in terms of computation time. This is why, prior to allocation of PV DGs, a sensitivity analysis can be

performed on the distribution network to find the buses that are the most sensitive to power losses after the injection of active and reactive power. The sensitivity of active power loss P_L with respect to active power injection is given in [13] as:

$$Sensitivity\ of\ P_L = \frac{\partial P_L}{\partial S} = \frac{P_L^{S+\Delta S} - P_L^S}{\Delta S} \qquad (18)$$

Where S is the active power injection, ΔS is the incremental change in S and P_L^S is the power loss value after injection of power S.

Therefore, for the optimization approach, the sensitivity of power loss P_L with respect to a small change in active injected power is calculated for each bus. Then, the buses are arranged in descending order based on their loss sensitivity values obtained. Afterward, the buses that are the most sensitive to power losses are chosen to be the candidate locations for optimal placement of PV DGs. After these steps are performed, the MOGA will run with the new reduced search space similar to what was explained in section III. 5 A.

C. Modified MOGA-LSF algorithm

As discussed in previous parts of section III. 5, the MOGA and MOGA-LSF algorithms will determine the optimal placement of PV DGs in the distribution network. However, the problem with these methodologies and most of the methodologies implemented in the literature, is that the candidate bus locations that achieve the best objective functions may not have good PV potentials. However, it is not possible to size based on the PV potential of the buses without considering the optimal sitting and sizing provided by the optimization methods. Hence, a modified version of the MOGA-LSF algorithm is proposed here. In this approach, both the feedback of the PV energy resource potentials and the system's optimal performance (minimum losses, cost, and voltage deviation) are simultaneously considered to solve the problem of optimal sitting and sizing of PV DG units in distribution networks.

After the sensitivity analysis is performed on all buses of the distribution network, each bus will have a corresponding sensitivity value. This value is combined with the maximum PV capacity of this bus using a 50% weight factor for each as shown in the equation below:

$$f(i) = 0.5 * LSF(i) + 0.5 * PV_{max}(i) \qquad (19)$$

Where $LSF(i)$ is the value of the loss sensitivity at bus i and $PV_{max}(i)$ is the maximum PV capacity of the bus as defined in table 3. The buses with the highest f values will be selected first. In this way, the PV potential of each bus is accounted for along with the sensitivity to power loss.

The flowchart below summarizes the optimization process of the modified MOGA-LSF:

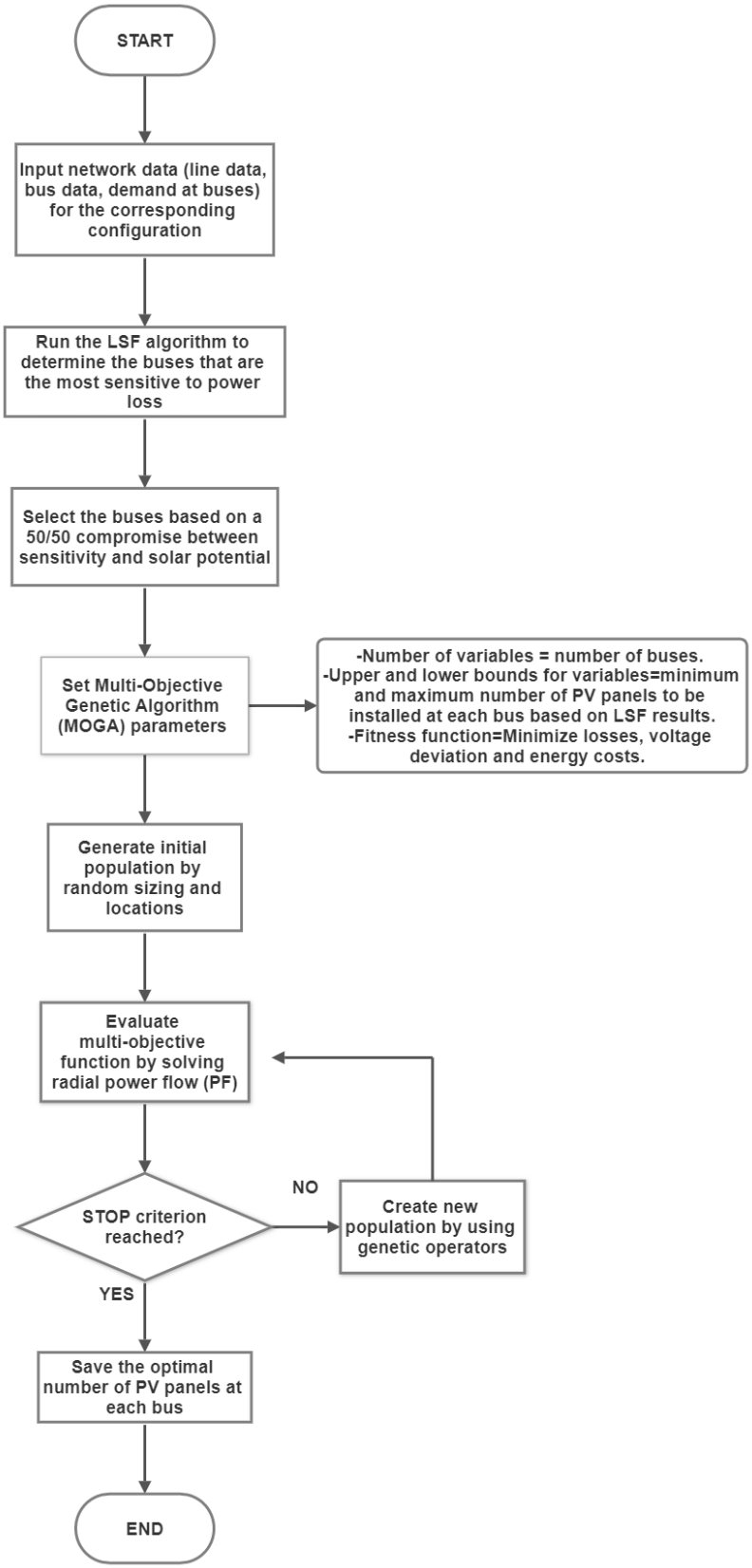

Figure 5: Modified MOGA-LSF algorithm methodology

IV. Results and discussion

The methodology was applied to the IEEE-15 bus distribution system whose detailed network data is given in section III. 3. The system is assumed to be operating under voltage limits of ± 10% with nominal thermal limits of 3 MVA for all the lines. All PV DG units are assumed to have a constant power factor of 0.9 lagging. The load profile of each configuration was deduced based on the load modeling methodology and the deduced active and reactive power demand of table 7 will be used. To calculate the cost objective function, the following levelized costs of electricity (LCOE) were considered: 20 c/kWh for the grid tariff and 8.5 c/kWh for the PV cost of energy. The optimization is carried out using the MATLAB platform incorporating features of the MATPOWER suite to solve the power flow at each iteration.

The results will be organized as follows; the first part is the optimization process carried out on each configuration on its own. The outcome of this part will be the optimal allocation of PV DGs for each of the six scenarios. In the second part, the optimal allocation of PV DGs on the configuration of the peak demand (C4) will be performed using the MOGA-LSF and the modified MOGA-LSF. The results of each algorithm will be compared to the optimal solution obtained using the traditional MOGA process. The third part will aim at determining the most optimum solution among the optimal solutions deduced in the first part by running each result on all the other configurations as detailed in section III. 5 A.

1. Optimization results for each configuration

In this part, the optimization algorithm will be applied to each configuration. However, since configurations C1, C5 and C6 are periods of zero solar irradiance, no optimization will be performed on them.

A. <u>Configuration C2</u>

The optimization process was run on configuration C2 where the total active and reactive power demand are 814 kW and 488 kVAR respectively. The figures below show the final population of obtained solutions or Pareto front considering power losses versus voltage deviation (fig. 6) and energy cost versus power losses (fig. 7):

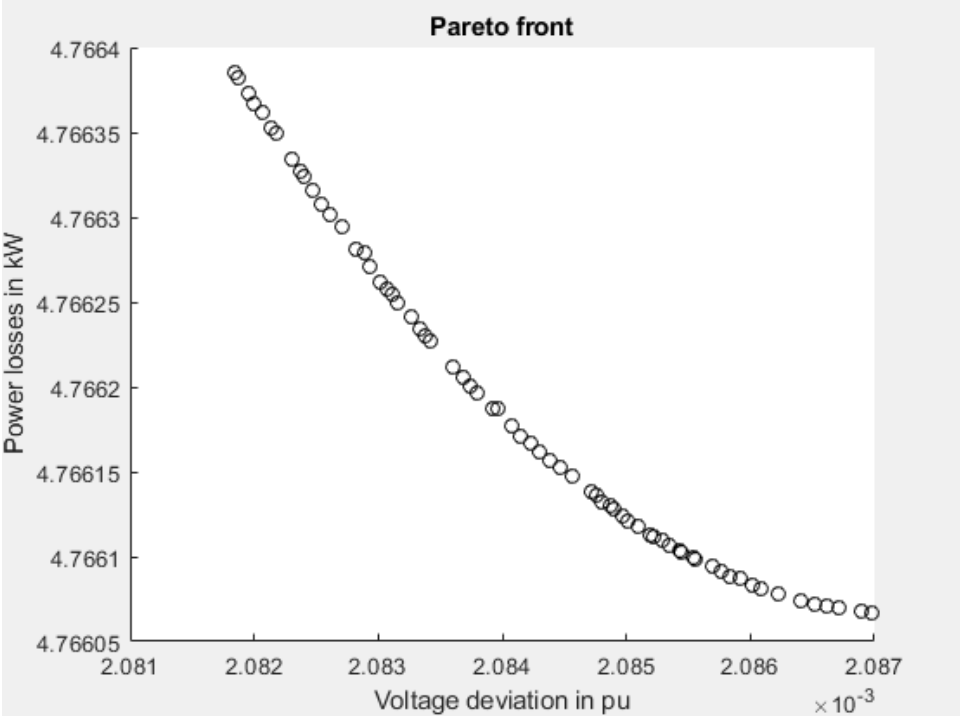

Figure 6: Pareto optimal solution set for PV DGs placement in C2 considering voltage deviation and power losses

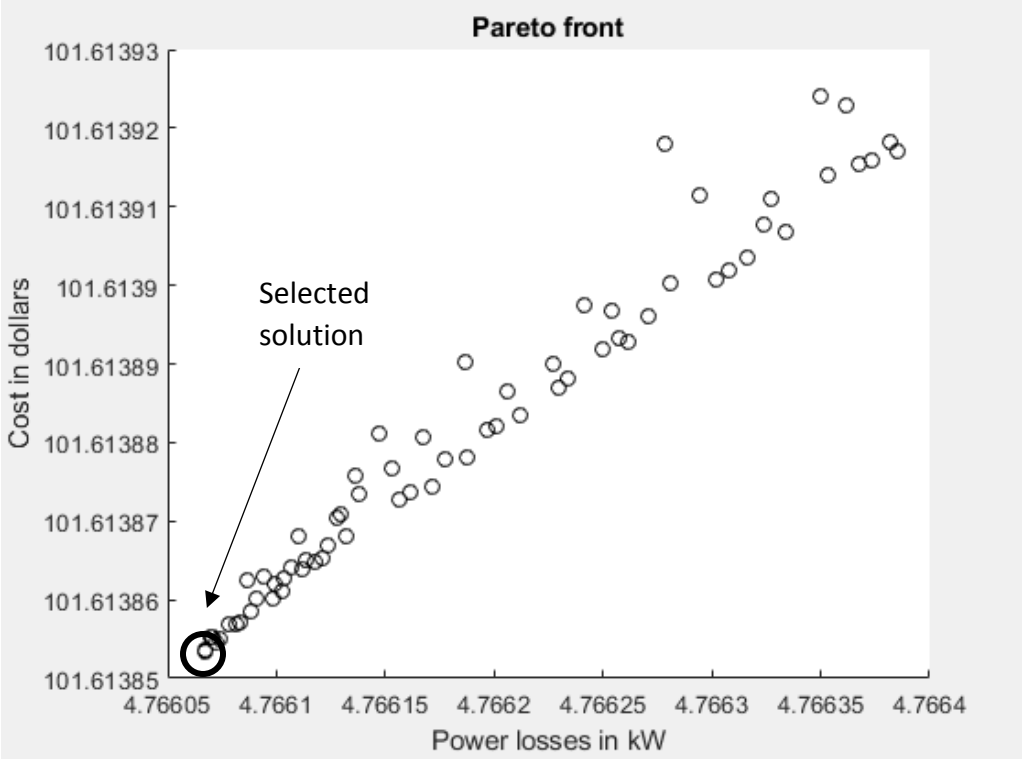

Figure 7: Pareto optimal solution set for PV DGs placement in C2 considering energy cost and power losses

It can be seen that the cost and power loss objective functions are non-conflicting. So, the solution that minimizes both functions is chosen.

The optimal number of PV panels to be placed at each bus along with the corresponding PV capacity to be installed are shown in the table below:

Table 8: Optimal number and capacity of allocated PV DGs for configuration C2

Bus number	Optimal number of panels (x)	PV capacity installed (in kw)
1	0	0
2	90	12.49
3	68	9.44
4	68	9.44
5	90	12.49
6	45	6.24
7	136	18.87
8	68	9.44
9	45	6.24
10	90	12.49
11	159	22.06
12	275	38.16
13	45	6.24
14	45	6.24
15	90	12.49
Total capacity		182.32 kW

The results of the optimization indicate that buses 12,11 and 7 are the buses with the highest PV capacity installed. Those three buses have the highest available area for PV placement (table 3) and are associated with moderate to high load demand. Hence, two conclusions can be drawn:

- The dispatched PV capacity will increase with the increase in solar PV generation. Buses with higher areas available for PV installation will be privileged over other buses with lower allowed installed PV capacity.

-The amount of PV power dispatched at each bus is dependent on the size of the load connected to it. Buses with higher loads connected to them will share more PV capacity, all other constraints being ignored. This is because, if a DG unit is placed near a large load, its contribution to minimizing network power losses will be high since a higher amount of load will be served. This is expected as the sole purpose of the optimal allocation is to decrease the power losses emanating from feeders being far away from load centers.

To assess the benefits of this optimal placement, the power flow was run on the optimized configuration and compared to the base case corresponding to no DGs installed. The results are shown in table 9 below:

Table 9: Optimization results for configuration C2 and base case

	Power losses (kW)	Energy cost(dollars)	Voltage deviation
No DGs	9.51	123.55	0.0042
With optimized PV DGs sizes and locations	4.77	101.63	0.0021

It is observed that the power losses of the system with PV-DGs are significantly reduced when compared to those of the system without PV (49.8 % decrease in losses from 9.51 kW to 4.77 kW). The energy cost also decreases from 123.5 $ to 101.6 $ equivalent to a 17.7% cost reduction. It is also evident that there is a positive relationship between power losses and cost as was noted from the Pareto front in figure 7. On the one hand, since the cost function includes fixed levelized costs of electricity for both the grid and the PV units, and since the cost of PV units is much lower than the cost of the grid, maximizing the PV penetration into the system will reduce the cost. On the other hand, the bigger the size of the PV DGs installed in the system, the bigger the decrease in the total power losses will be (considering limits on penetration levels are respected). Hence, the optimal allocation of PV DGs will have both technical and economic benefits.

Moreover, figure 8 shows the voltage profile of the system for both the base case associated with no DGs installed and the case of optimized PV DGs capacities installed:

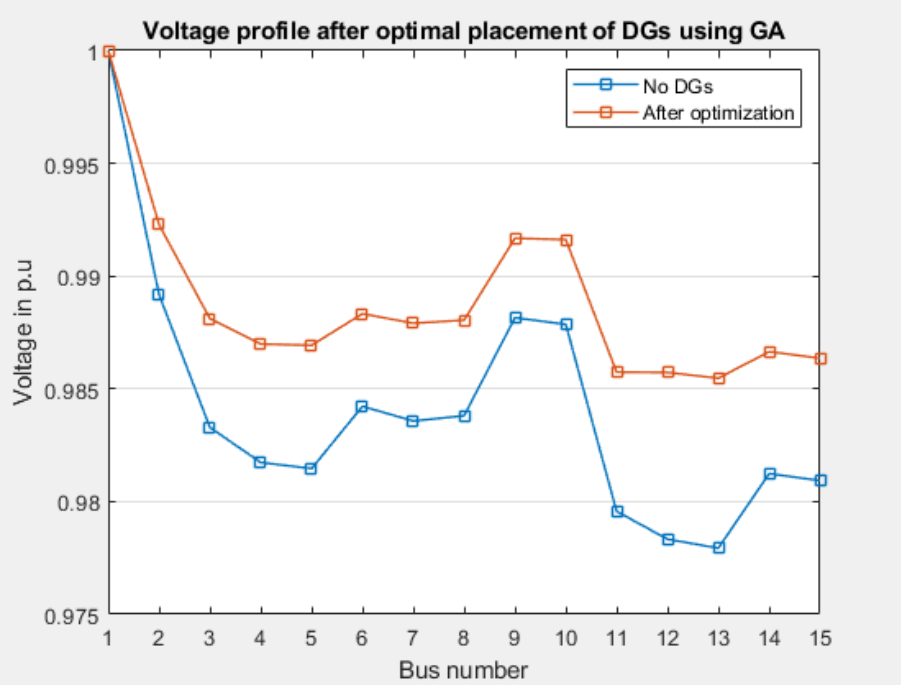

Figure 8: Voltage profiles before and after optimization for C2

The figure indicates an enhancement of the voltage profile when PV DGs are optimally placed as compared to the no-DG case.

B. Configuration C3

The optimization process was run on configuration C3 where the total active and reactive power demand are 608 kW and 350 kVAR respectively. Figures 9 and 10 show the final population of obtained solutions considering power losses and voltage deviation then power losses and energy cost:

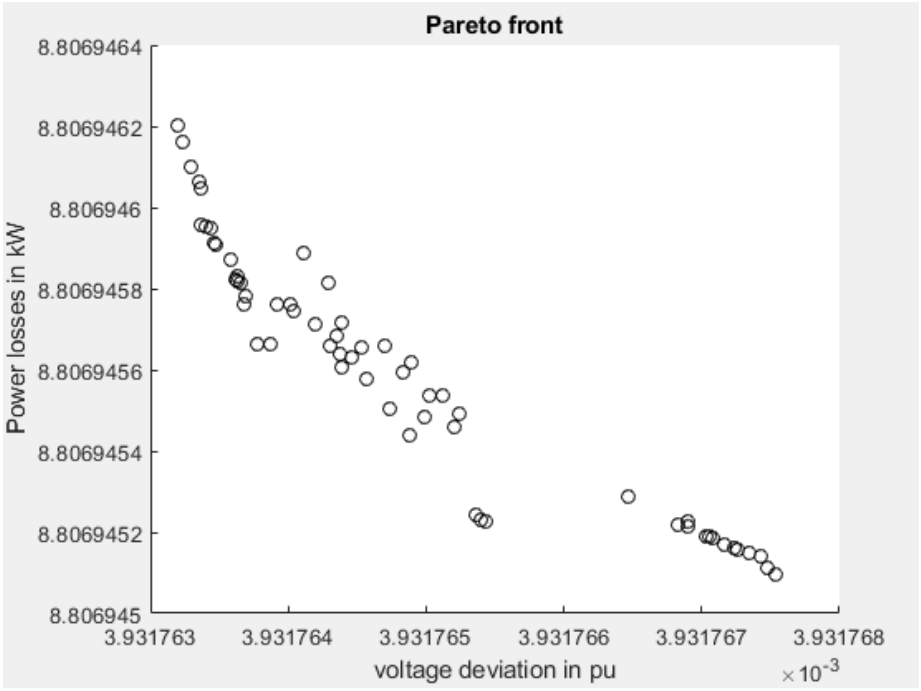

Figure 9: Pareto optimal solution set for PV DGs placement in C3 considering voltage deviation and power losses

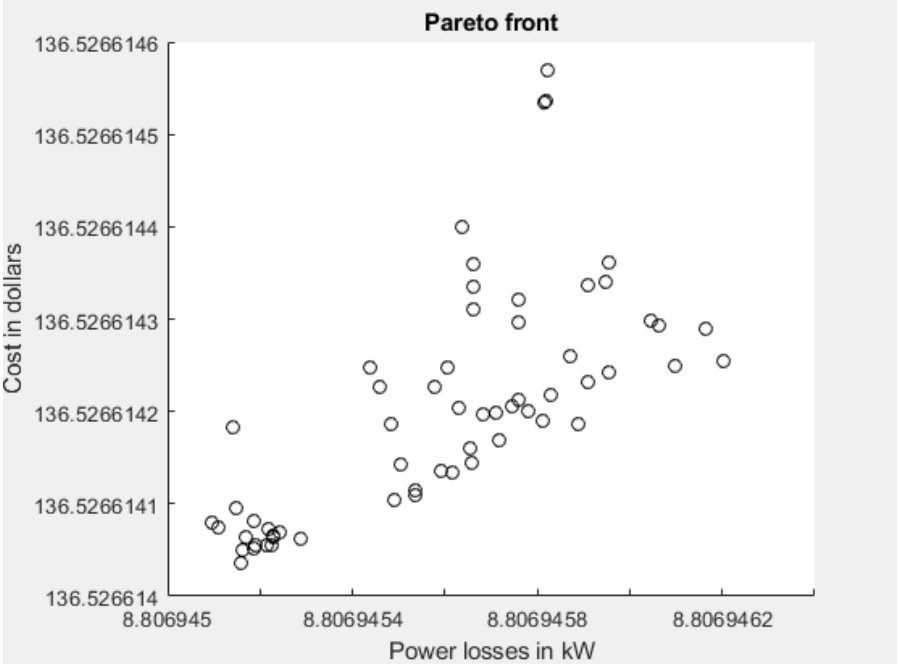

Figure 10: Pareto optimal solution set for PV DGs placement in C3 considering energy cost and power losses

The optimal number of PV panels to be placed at each bus along with the corresponding PV capacity to be installed are shown in the table below:

Table 10: Optimal number and capacity of allocated PV DGs for configuration C3

Bus number	Optimal number of panels (x)	PV capacity installed (in kw)
1	0	0
2	75	15.34
3	77	15.75
4	104	21.27
5	80	16.36
6	39	7.98
7	105	21.47
8	54	11.04
9	46	9.41
10	81	16.57
11	154	31.49
12	97	19.84
13	99	20.25
14	94	19.22
15	84	17.18
Total capacity		243.16 kW

Buses 11,7,13 and 4 have the largest PV capacity (94 kW) and buses 6 and 9 have the lowest ones (17.39 kW). It is noted that the installed PV capacity is most importantly limited by the PV penetration limit of 30% set as one of the optimization constraints. As it was deduced for configuration 2, buses associated with a high available area for PV installation and high demand, resulted in high installed PV capacity after the optimization algorithm was executed.

To assess the benefits of this optimal placement, the power flow was run on the optimized configuration and compared to the base case corresponding to no DGs installed. The results are shown in 1table 11 below:

Table 11: Optimization results for configuration C3 and base case

	Power losses (kW)	Energy cost(dollars)	Voltage deviation
No DGs	17.42	166.34	0.0079
With optimization	8.84	136.66	0.0039

Again, power losses decreased from 17.4 kW in the case of no DGs installed, to 8.84 kW after the optimal allocation of PV DGs. This corresponds to about a 49% loss reduction. The cost also decreased by 17.8 %. The voltage deviation also improved from 0.0079 pu to 0.0039 pu.

Figure 11 shows the enhancement in the voltage profile achieved after the optimal allocation of the PV DGs.

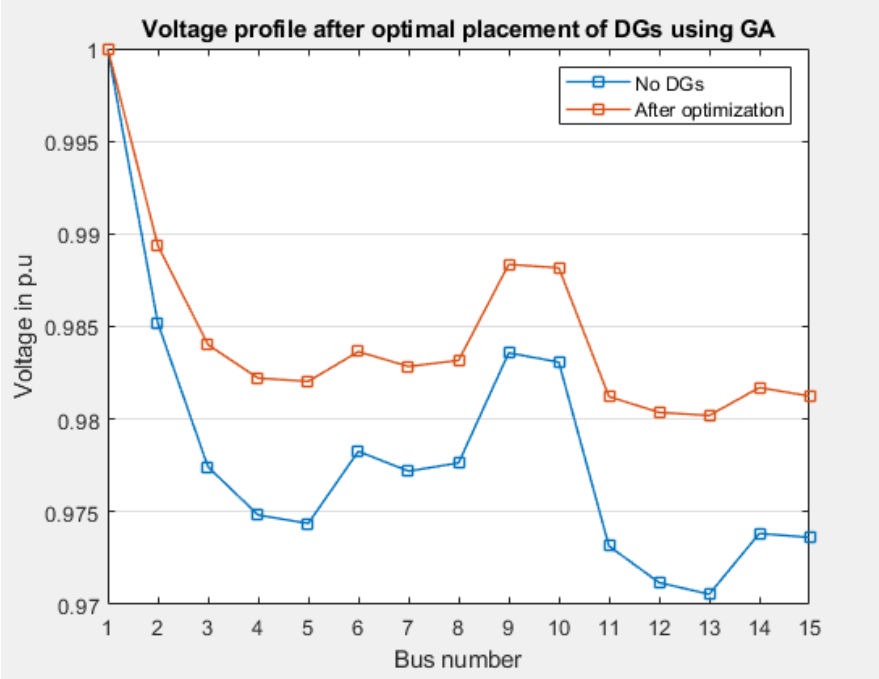

Figure 11: Voltage profiles before and after optimization for C3

C. Configuration C4

The optimization process was run on configuration C4 where the total active and reactive power demand are their peak value of 1226 kW and 766 kVAR respectively. Figures 12 and 13 below show the Pareto fronts obtained for the three objective functions:

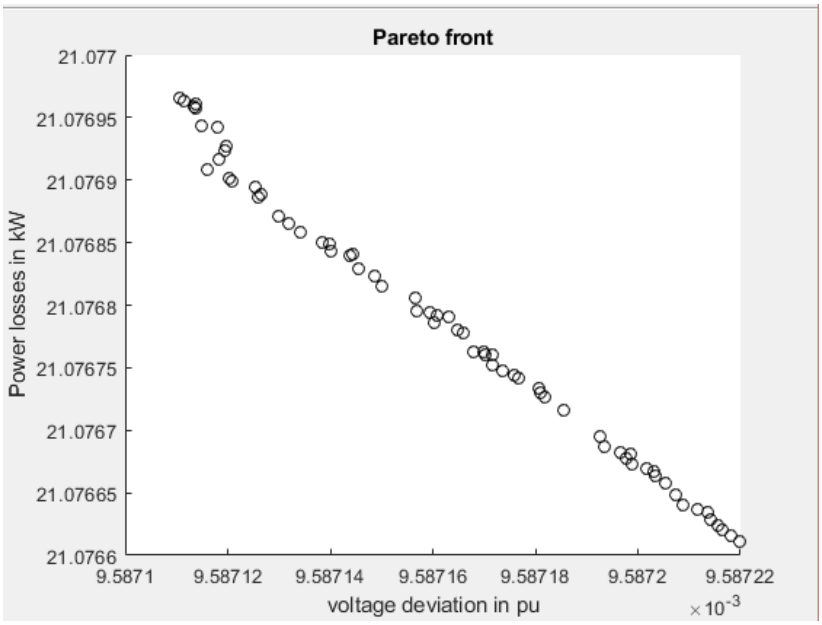

Figure 12: Pareto optimal solution set for PV DGs placement in C4 considering voltage deviation and power losses

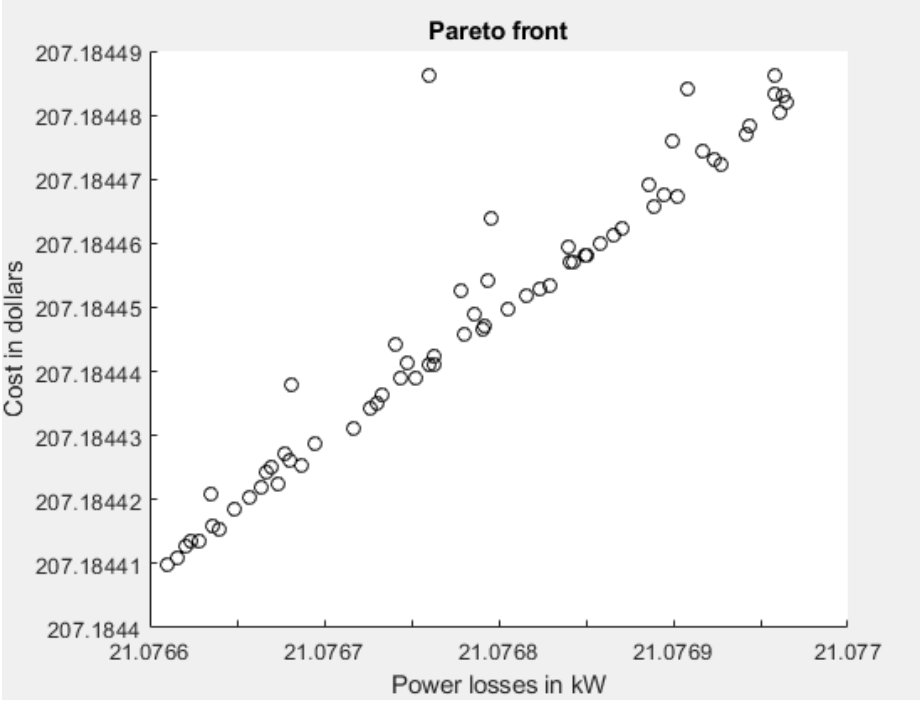

Figure 13: Pareto optimal solution set for PV DGs placement in C4 considering energy cost and power losses

The optimal number of PV panels to be placed at each bus along with the corresponding PV capacity to be installed are shown in the table below:

Table 12: Optimal number and capacity of allocated PV DGs for configuration C4

Bus number	Optimal number of panels (x)	PV capacity installed (in kw)
1	0	0
2	236	21.90
3	290	26.92
4	323	29.98
5	378	35.08
6	187	17.36
7	404	37.50
8	262	24.32
9	182	16.89
10	262	24.32
11	405	37.59
12	327	30.35
13	187	17.36
14	176	16.34
15	340	31.56
Total capacity		367.45 kW

The largest PV capacity (142 kW) has been installed at buses 7,11,5 and 15. Again for this configuration, the buses with the highest installed capacity are associated with the highest available PV capacity and the highest demand. This is again caused by the dispatched PV power increasing with both load demand and solar potential.

To assess the benefits of this optimal placement, the power flow was run on the optimized configuration and compared to the base case corresponding to no DGs installed. The results are shown in table 13 below:

Table 13: Optimization results for configuration C4 and base case

	Power losses (kW)	Energy cost(dollars)	Voltage deviation
No DGs	41.3	253.54	0.0188
With optimization	21.097	207.24	0.0096

The power losses decreased from 41.3 kW in the case of no DGs installed to 21 kW when PV-DGs were optimally placed which is equivalent to a 48.9 % loss reduction. The energy cost also decreased by about 18.3 %. Again here, minimizing cost is tightly related to minimizing losses.

The voltage profile after optimal siting and sizing of the PV DGs is also improved as deduced from figure 14:

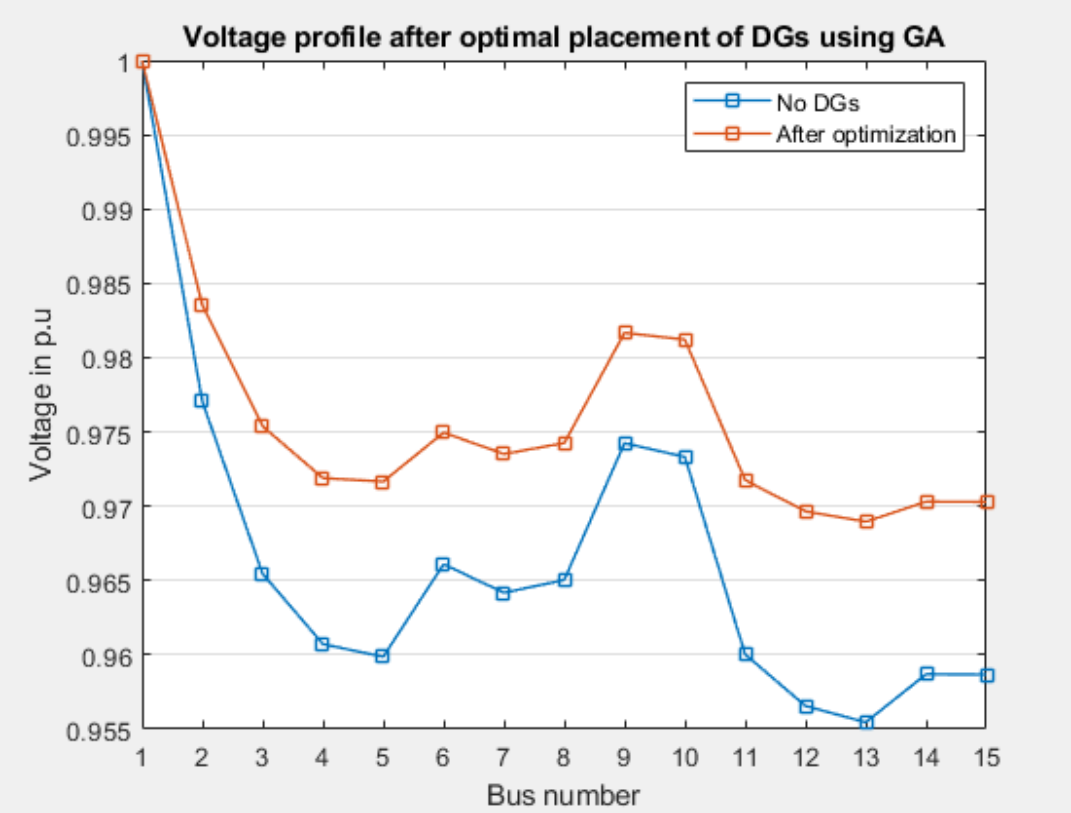

Figure 14: Voltage profiles before and after optimization for C4

Comparing the three individual configurations, two important conclusions can be drawn:

-Buses 11 and 7 have the largest installed PV capacity for all three configurations. This can be explained by the fact that no matter the configuration, these buses have a high area available for PV installation.

-The size and location of PV DGs differ between the three considered configurations. This indicates that the time-varying load model plays a critical role in the optimal allocation problem since each load profile will result in different dispatched PV capacities. This further shows that both peak load and fixed load optimizations, done extensively in the literature, would not provide accurate results.

2. Hybrid MOGA-LSF and modified MOGA-LSF results on configuration C4

As mentioned in section III. 5, a sensitivity analysis is conducted on the buses to reduce the search space and choose between a set of candidate locations. The results of the LSF are shown in the table below:

Table 14: Buses ranked in descending order based on their calculated LSF values

Bus Number	LSF	PV max capacity (kW)
7	-0.0621	63
8	-0.0558	31.5
6	-0.0549	21
3	-0.0538	31.5
4	-0.0498	31.5
2	-0.0461	42
14	-0.0376	21
15	-0.0358	42
5	-0.0343	42
10	-0.0335	42
12	-0.0309	42
11	-0.0299	63
13	-0.0229	21
9	-0.0193	21
1	0.0000	0

From table 14, only buses 7,8,6,3,4,2,14, and 15 were considered for optimal allocation of PV DGs as being the most sensitive to changes in injected power. Figure 15 shows the real power loss sensitivity with respect to real power injection:

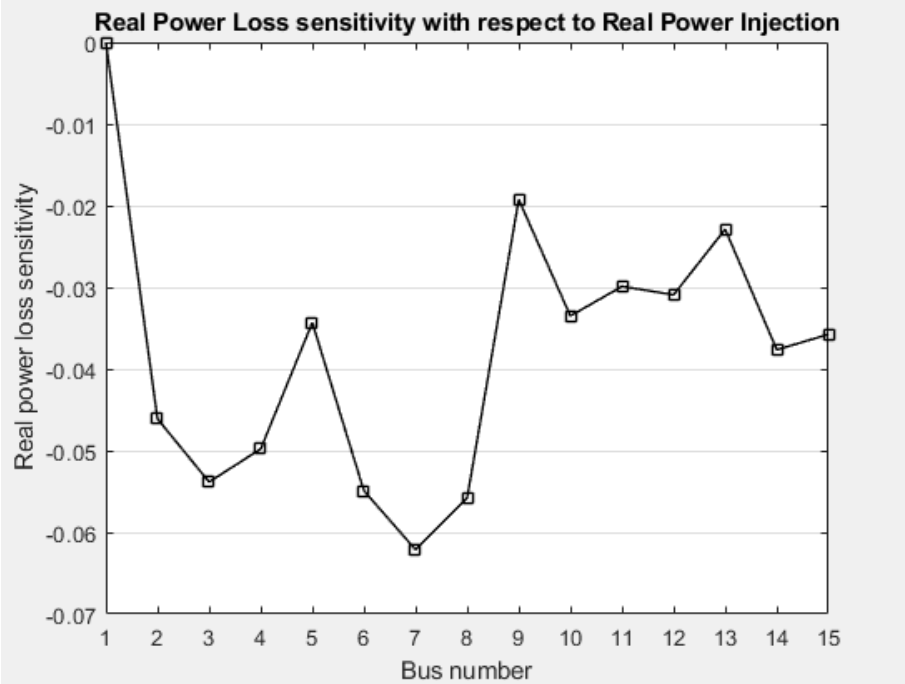

Figure 15: Sensitivity analysis conducted on the 15-bus distribution system

Running the optimization with the candidate buses resulted in one optimal solution. The optimal number of PV panels to be placed at each bus along with the corresponding PV capacity to be installed are shown in the table below:

Table 15: Optimal number and capacity of allocated PV DGs for configuration C4 using MOGA-LSF

Bus number	Optimal number of panels (x)	PV capacity installed (in kw)
1	0	0
2	345	32.02
3	236	21.90
4	301	27.94
5	0	0
6	180	16.71
7	629	58.38
8	314	29.14
9	0	0
10	0	0
11	0	0
12	0	0
13	0	0
14	166	15.41
15	379	35.18
Total capacity		236.67 kW

For the modified MOGA-LSF, solar PV assessment was included when choosing the candidate buses for optimal allocation. The table below shows the combined scores of LSF, and capacity computed for each bus:

Table 16: Buses ranked in descending order based on their score values

Bus number	LSF	Max capacity	0.5*LSF+0.5*capacity
1	0	0	0.00
6	-0.0549	21	10.47
14	-0.0376	21	10.48
13	-0.0229	21	10.49
9	-0.0193	21	10.49
8	-0.0558	31.5	15.72
3	-0.0538	31.5	15.72
4	-0.0498	31.5	15.73
2	-0.0461	42	20.98
15	-0.0358	42	20.98
5	-0.0343	42	20.98
10	-0.0335	42	20.98
12	-0.0309	42	20.98
7	-0.0621	63	31.47
11	-0.0299	63	31.49

From table 16, buses 6,14,13,9,8 and 3 were discarded having the lowest LSF/PV capacity. Two optimal solutions were found. The one that achieved the lower power losses was privileged over the other. The optimal number of PV panels to be placed at each bus along with the corresponding PV capacity to be installed are shown in the table below:

Table 17: Optimal number and capacity of allocated PV DGs for configuration C4 using modified MOGA-LSF

Bus number	Optimal number of panels (x)	PV capacity installed (in kw)
1	0	0
2	392	36.38
3	0	0
4	312	28.96
5	403	37.40
6	0	0
7	586	54.39
8	0	0
9	0	0
10	397	36.85
11	458	42.51

12	427	39.63
13	0	0
14	0	0
15	415	38.52
Total capacity		314.64 kW

To assess the efficiency of the two implemented algorithms, the power losses, energy cost, and voltage deviation obtained with each of these two algorithms were compared to the results obtained using the traditional MOGA. The outcomes of each algorithm are summarized in the table below:

Table 18: Optimization results for configuration C4 using MOGA, MOGA-LSF, and modified MOGA-LSF

	Power losses (kW)	**Energy cost(dollars)**	**Voltage deviation**
MOGA	21.097	207.24	0.0096
MOGA-LSF	28.003	223.66	0.01301
Modified MOGA-LSF	23.76	213.85	0.0108

First, it can be observed that the MOGA provides better results than both hybrid techniques for all the objective functions. The MOGA-LSF achieves the highest amount of power losses and cost (28 kW and 224 $ respectively) followed by the modified MOGA-LSF with 23.7 kW of losses and 214$ for energy cost.

Figure 16 shows the voltage profiles obtained for each of the three algorithms, again showing the superiority of the MOGA over the two implemented algorithms:

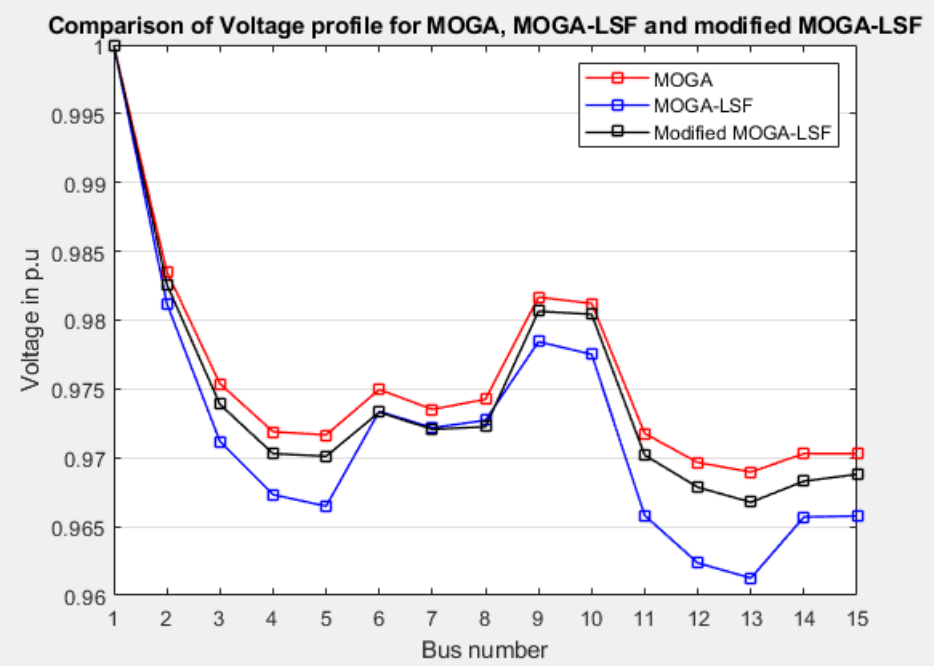

Figure 16: Voltage profile of configuration C4 for the three optimization algorithms

Even though the results of the newly implemented algorithms (MOGA-LSF and modified MOGA-LSF) were deceiving, important conclusions can be drawn:

1. The modified MOGA-LSF achieved better results than the MOGA-LSF with a 42.5% loss reduction compared to a 32% loss reduction only for the MOGA-LSF algorithm. This confirms the initial hypothesis that the PV assessment of buses is of primary importance when the optimal allocation of PV DGs is concerned. Choosing the buses with the highest PV potential as candidates improved the results and confirms that solar potential has a big influence on the installation of PV units in distribution networks.

2. The superiority of the MOGA over the implemented algorithms is caused by the direct relationship between the size of DGs and the power losses. As it was established from the individual optimizations performed on configurations 2,3 and 4 in section IV. 1, the bigger the dispatched capacity of the PV DGs installed, the bigger the benefits will be on the total power losses and consequently the energy cost. Since both the MOGA-LSF and the modified MOGA-LSF restrict the allocation to a reduced number of buses, the total installed DG capacity will be less resulting in lower loss percentages and cost reductions.

Moreover, this raises a question already highlighted by the authors in [3]. For the two hybrid techniques, the PV DGs were placed in a restricted number of locations (8 allowed locations), but they had high capacities (reaching 54 kW at bus 7 for the modified MOGA-LSF), whereas, for the MOGA, more locations were considered for the DGs (14 locations as the slack bus is excluded) with lower capacities (maximum capacity of 37 kW installed at bus 7). This shows that spreading the DG capacities by connecting DGs of smaller sizes in more locations resulted in higher improvements in losses and costs. So, the results reveal what was yet unclear in the findings of [3]: the improvements done by optimal allocation of PV DGs increase by considering more locations. Hence, as suggested in [3], distribution network operators should promote micro-generation for customers that are far away from main feeders because spreading DG capacity further improves the benefits of their installation in the network.

3. Choice of the optimal solution

Now that the optimal locations and sizes were found for each of configurations C2, C3, and C4 (tables 8, 9, and 12), the next step will aim to find the optimum solution among the three solutions obtained. For this purpose, the total average power losses and total average energy cost were calculated as the weighted sum of all hourly power losses or hourly energy costs obtained in each configuration considering one of the three optimal solutions as fixed.

Table 19 shows the results obtained for the base case when no PV DGs were installed. The total average losses were 16.3 kW, and the total average energy cost was 148.42 dollars. As expected, as the load demand increases, the power losses increase as distribution lines become heavily loaded. Hence, it's during configuration C4 of the peak that the highest amount of power losses (165 kW) and the highest energy cost (1014$) are observed.

Tables 20-22 indicate the total average losses, total average cost, and the percentage PV penetration obtained when considering the result of siting and sizing in configuration C2, then C3 then C4 as optimal:

Table 19: Total average losses and total average cost for the base case

Base case	Total losses (in kW)	Cost (in dollars)	Hours	Total average losses (in kW)	Total average cost (in $)	% PV penetration
Configuration C01	4.49	84.69	7.00	31.44	592.80	0
Configuration C02	9.51	123.55	4.00	38.03	494.20	0
Configuration C03	17.42	166.34	3.00	52.26	499.02	0
Configuration C04	41.29	253.54	4.00	165.18	1014.16	0
Configuration C05	23.15	191.92	4.00	92.60	767.68	0
Configuration C06	5.84	97.08	2.00	11.69	194.17	0
Total				**16.30**	**148.42**	

Table 20: Total average losses and total average cost using the solution of C2

Optimum configuration C2	Total losses (in kW)	Cost (in dollars)	Hours	Total average Losses (in kW)	Total average cost (in $)	% PV penetration
Configuration C21	4.43	84.32	7	30.99	590.24	0.73
Configuration C22	4.77	101.63	4	19.08	406.52	29.98
Configuration C23	8.08	133.57	3	24.25*	400.71*	33.00
Configuration C24	33.65	237.98	4	134.59*	951.92*	9.94
Configuration C25	23.15	191.92	4	92.60	767.68	0
Configuration C26	5.84	97.08	2	11.69	194.17	0
Total				**13.05**	**137.97**	

Table 21: Total average losses and total average cost using the solution of C3

Optimum configuration C3	Total losses (in kW)	Cost (in dollars)	Hours	Total average losses (in kW)	Total average cost (in $)	% PV penetration
Configuration C31	4.43	84.36	7	31.04	590.49	0.66
Configuration C32	5.18	103.71	4	20.72	414.84	27.12
Configuration C33	8.84	136.66	3	26.51*	409.98*	29.86
Configuration C34	34.37	239.46	4	137.46*	957.84*	9
Configuration C35	23.15	191.92	4	92.60	767.68	0
Configuration C36	5.84	97.08	2	11.69	194.17	0
Total				**13.33**	**138.96**	

Table 22: Total average losses and total average cost using the solution of C4

Optimum configuration C4	Total losses (in kW)	Cost (in dollars)	Hours	Total average losses (in kW)	Total average cost (in $)	% PV penetration
Configuration C41	4.31	83.58	7.00	30.15	585.08	2.21
Configuration C42	0.38	58.55	4.00	1.51	234.20	90.32
Configuration C43	0.38	69.83	3.00	1.14	209.48	99.43
Configuration C44	21.10	207.24	4.00	84.39	828.96	29.96
Configuration C45	23.15	191.92	4.00	92.60	767.68	0
Configuration C46	5.84	97.08	2.00	11.69	194.17	0
Total				**9.23**	**117.48**	

First, the results reveal that regardless of the solution chosen to allocate the PV DGs for all the configurations, there is a significant reduction in both the average power losses and the average energy losses.

Second, the optimal number and capacity of the allocated PV DGs for configuration C2 provide better results in configuration C3 than its optimal solution (C23 compared to C33). For instance, for scenario C23, the power losses are 24.25 kW compared to 26.51 kW for scenario C33 which corresponds to an 8.5 % improvement in losses. The cost also improved by 2.3%. The fact that the solution of configuration C2 achieves better results on configuration C3 is caused by the higher amount of solar irradiance in configuration C3. During this period, the highest solar output is obtained. So, the panels that are installed will provide a higher output. Hence, even though the number of panels installed in C2 is lower than in C3, it will be compensated by a higher solar irradiance that will increase the capacity of the PV installed.

Third, at first sight, the optimal solution obtained in configuration C4 of the peak appears to achieve the lowest total average losses of 9.23 kW and the lowest average cost of 117.48 dollars. This is caused by the fact that the number of panels installed in configuration C4 is the highest since the load during this period is the highest. So, a higher PV DG capacity will be installed in both configurations C3 and C4. Since it was already established that the bigger the capacity of PV DGs installed in the system, the bigger the impact on total power losses and cost will be, these results are expected. Figure 17 reveals that the adopted solution of configuration C4 achieves 43% power loss reduction and 20.84% energy cost reduction from the base case of no DGs installed compared to only 18.19% loss reduction and 6.4% cost reduction if the solution of configuration C3 is adopted.

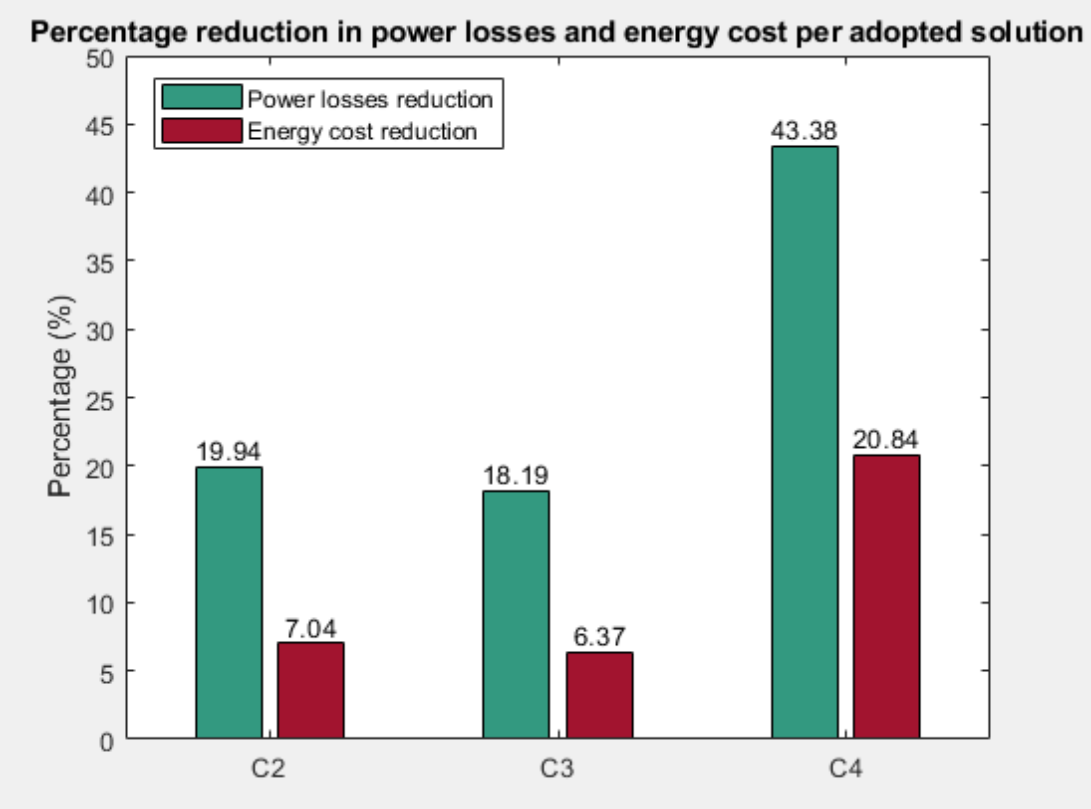

Figure 17: Percentage of power losses and energy cost reductions for each of the three adopted solutions

However, adopting the solution of configuration C4 is not practically possible. The detailed results of configuration C4 provided in table 22 reveal that the 30% PV penetration level constraint is by far exceeded in both scenarios C42 and C43 (PV penetration of 90% for C42 and 99% for C43) rendering the solution of C4 unacceptable. The solution of the peak is oversized for hours corresponding to periods C2 and C3 where the demands are much lower (1.5 times lower for C3 and 2 times lower for C4). This may not be beneficial because stability issues will start to appear, and losses could increase beyond expected if the surplus in generation becomes more pronounced.

The alternative would be to select the solution of configuration C2 as the second-best solution in terms of loss reduction and cost. Note that the PV penetration level in scenario C23 is 33% which is slightly higher than 30%. If there is a strict limitation on the PV penetration level, then this solution should also be discarded and the solution of configuration C3 will be selected. However, since this penetration level is still below the 40% stability limit, then the solution of C2 will be the most optimal solution to be adopted on all the configurations as it achieves power losses and energy cost reductions while not breaching the technical constraints of the network.

Based on these results, an important conclusion can be drawn concerning the siting and sizing at peak load. Trying to search for the optimal solution during the peak load hour as it was done extensively in the literature, will lead to an overestimation of the benefits of the optimal

allocation of PV DGs. What appeared to be a 43% reduction in power losses based on peak load optimization turned out to be a 20% reduction in losses only when technical constraints are considered. Therefore, even though the peak power approach requires low computation time, it is not precise enough in two aspects:

-First, as discussed in section IV. 1, this approach fails to represent the time-varying nature of the load which will affect the siting and sizing solution.

-Second, it overestimates the benefits of finding the optimal sizes of the PV DGs by oversizing in periods where the demand is lower and consequently increasing the risks of technical issues arising from the surplus of generation and the high penetration levels.

V. Conclusion and future works

In this work, a new methodology that uses the Multi-Objective Genetic Algorithm (MOGA) is proposed for the optimal allocation of PV-based distributed generation units (PV-DGs) in distribution networks. The method aims at minimizing active power losses, voltage deviations, and energy costs using a practical model that considers both the solar potential of each bus and variable load classifications. The major findings of this paper are:

-The larger the installed PV DGs capacity, the higher the benefits in terms of minimization of power losses and energy costs and improvement of the voltage profile.

-Solar PV assessment plays a major role in the siting and sizing of PV DGs justified by the results of the modified MOGA-LSF being better compared to the MOGA-LSF results.

-The MOGA-LSF and the modified MOGA-LSF are less efficient than the MOGA in terms of finding the optimal solution but highlight the advantages of spreading DG capacity.

-The work shows the weakness of the peak hour optimization mainly since it fails to capture the time variations of the load that affect the optimization results and it overestimates the benefits of the optimal allocation of the PV units in distribution networks.

The contributions of the proposed PV DGs planning technique are:

-The proposed methodology succeeds in reducing the power losses, energy costs, and voltage deviations of the distribution system at hand while guaranteeing no violation of any system constraints under all load configurations. Even though lower benefits are achieved, the results are more realistic and more considerate of the technical constraints of the system by keeping PV penetration levels and voltage profile levels within acceptable limits.

-The method proposes a practical load model that captures the time-varying nature of the loads and their mixed types (residential, commercial, and industrial) for each bus of the network.

Considering different types of loads will affect the allocation of PV units in the distribution system and contribute to more realistic results.

-To our knowledge, the MOGA-LSF hybrid algorithm was not implemented on the problem of optimal allocation of PV DGs in distribution networks in any of the surveyed literature.

Future works will include:

-Modeling the seasonal variations of the load. Currently, the work at hand models only one summer day in the year. Representing the three other seasons would contribute to more realistic results and the load profile will be more accurate.

-Expanding the cost optimization function. Currently, constant levelized costs of energy are considered for the PV DGs regardless of the energy produced. A major improvement will be to use a variable PV DG cost at each bus of the distribution system calculated based on the energy generated per year. Moreover, the cost function can accommodate additional terms such as system reinforcement costs and incentive/penalty factors for reducing/increasing losses.

3. Include storage mainly in configurations C1, C5 and C6 where no solar irradiance is available.

4. Include non-renewable DG sources to further highlight the benefits of renewable DGs.

5. Implementing more powerful optimization techniques than the MOGA such as the particle-swarm optimization (PSO) and the ant-lion optimization (ALO) to reach yet better optimal results with lower computation time.

References

[1] A. Arabali, M. Ghofrani, J. B. Bassett, My Pham, and M. Moeini-Aghtaei, “Chap 7: Optimum sizing and siting of renewable-energy-based DG units in distribution systems,” in *Optimization in renewable energy systems: Recent perspectives*, Oxford: Butterworth-Heinemann, 2017, pp. 233–277.

[2] O. Badran, S. Mekhilef, H. Mokhlis, and W. Dahalan, “Optimal reconfiguration of distribution system connected with Distributed Generations: A Review of different methodologies,” *Renewable and Sustainable Energy Reviews*, vol. 73, pp. 854–867, 2017.

[3] Harrison, G, Piccolo, A, Siano, P & Wallace, R 2008, 'Hybrid GA and OPF evaluation of network capacity for distributed generation connections', *Electric Power Systems Research*, vol. 78, no. 3, pp. 392–398

[4] A. Selim, S. Kamel, A. A. Mohamed, and E. E. Elattar, “Optimal allocation of multiple types of distributed generations in radial distribution systems using a hybrid technique,” *Sustainability*, vol. 13, no. 12, p. 6644, 2021.

[5] Y. M. Atwa and E. F. El-Saadany, “Probabilistic approach for optimal allocation of wind-based distributed generation in Distribution Systems,” IET Renewable Power Generation, vol. 5, no. 1, pp. 79-88, 2011.

[6] P. Chen, P. Siano, B. Bak-Jensen, and Z. Chen, “Stochastic optimization of wind turbine power factor using stochastic model of wind power,” *IEEE Transactions on Sustainable Energy*, vol. 1, no. 1, pp. 19–29, 2010.

[7] P. Siano and G. Mokryani, “Evaluating the benefits of optimal allocation of wind turbines for distribution network operators,” *IEEE Systems Journal*, vol. 9, no. 2, pp. 629–638, 2015.

[8] P. Siano and G. Mokryani, “Assessing wind turbines placement in a distribution market environment by using particle swarm optimization,” *IEEE Transactions on Power Systems*, vol. 28, no. 4, pp. 3852–3864, 2013.

[9] G. Mokryani and P. Siano, “Strategic placement of distribution network operator owned wind turbines by using market-based Optimal Power Flow,” *IET Generation, Transmission & Distribution*, vol. 8, no. 2, pp. 281–289, 2014.

[10] A. Naderipour, Z. Abdul-Malek, M. W. Mustafa, and J. M. Guerrero, “A multi-objective artificial electric field optimization algorithm for allocation of wind turbines in Distribution Systems,” *Applied Soft Computing*, vol. 105, p. 107278, 2021.

[11] V. Vita, “Development of a decision-making algorithm for the optimum size and placement of distributed generation units in Distribution Networks,” *Energies*, vol. 10, no. 9, p. 1433, 2017.

[12] R. K. Samala and K. Mercy Rosalina, “Optimal allocation of multiple photo-voltaic and/or wind-turbine based distributed generations in radial distribution system using hybrid technique with Fuzzy Logic Controller,” *Journal of Electrical Engineering & Technology*, vol. 16, no. 1, pp. 101–113, 2020.

[13] Gopiya Naik. S, D.K. Khatod and M.P. Sharma, Optimal Allocation of Dispatchable and Non-Dispatchable DG Units In Distribution Networks. International Journal of Electrical Engineering & Technology, 8(6), 2017, pp. 29–56,2016.

[14] M. Kefayat, A. Lashkar Ara, and S. A. Nabavi Niaki, “A hybrid of ant colony optimization and artificial bee colony algorithm for probabilistic optimal placement and sizing of distributed energy resources,” *Energy Conversion and Management*, vol. 92, pp. 149–161, 2015.

[15] A. S. Hassan, Y. Sun, and Z. Wang, “Water, energy and food algorithm with optimal allocation and sizing of renewable distributed generation for power loss minimization in distribution systems (WEF),” *Energies*, vol. 15, no. 6, p. 2242, 2022.

[16] H. Hassanzadeh Fard and A. Jalilian, “Optimal sizing and siting of renewable energy resources in distribution systems considering time varying electrical/heating/cooling loads using PSO algorithm,” *International Journal of Green Energy*, vol. 15, no. 2, pp. 113–128, 2018.

[17] N. Haghdadi, B. Asaei, and Z. Gandomkar, “Clustering-based optimal sizing and siting of photovoltaic power plant in Distribution Network,” *2012 11th International Conference on Environment and Electrical Engineering*, 2012.

[18] M. Duong, T. Pham, T. Nguyen, A. Doan, and H. Tran, “Determination of optimal location and sizing of solar photovoltaic distribution generation units in radial distribution systems,” *Energies*, vol. 12, no. 1, pp. 174, 2019.

[19] M. Bazrafshan, L. Yalamanchili, N. Gatsis, and J. Gomez, “Stochastic planning of distributed PV Generation,” *Energies*, vol. 12, no. 3, pp. 459, 2019.

[20] M. D. Hraiz, J. A. Garcia, R. Jimenez Castaneda, and H. Muhsen, “Optimal PV size and location to reduce active power losses while achieving very high penetration level with improvement in voltage profile using modified Jaya algorithm,” *IEEE Journal of Photovoltaics*, vol. 10, no. 4, pp. 1166–1174, 2020.

[21] A. Paz-Rodríguez, J. F. Castro-Ordoñez, O. D. Montoya, and D. A. Giral-Ramírez, “Optimal integration of photovoltaic sources in distribution networks for daily energy losses minimization using the vortex search algorithm,” *Applied Sciences*, vol. 11, no. 10, pp. 4418, 2021.

[22] O. D. Montoya, D. A. Giral-Ramírez, and J. C. Hernández, “Efficient integration of PV sources in distribution networks to reduce annual investment and operating costs using the modified arithmetic optimization algorithm,” *Electronics*, vol. 11, no. 11, pp. 1680, 2022.

[23] O. D. Montoya, L. F. Grisales-Noreña, and C. A. Ramos-Paja, “Optimal allocation and sizing of PV generation units in distribution networks via the Generalized Normal distribution optimization approach,” *Computers*, vol. 11, no. 4, pp. 53, 2022.

[24] R. O. Bawazir and N. S. Cetin, “Comprehensive overview of optimizing PV-DG allocation in power system and Solar Energy Resource Potential Assessments,” *Energy Reports*, vol. 6, pp. 173–208, 2020.

[25] P. Dakic and D. Kotur, “Optimal placement of photovoltaic systems from the aspect of minimal power losses in distribution network based on genetic algorithm,” *Thermal Science*, vol. 22, no. Suppl. 4, pp. 1157–1170, 2018.

[26] M. Ahmadi, M. E. Lotfy, R. Shigenobu, A. Yona, and T. Senjyu, “Optimal sizing and placement of rooftop solar photovoltaic at Kabul City Real Distribution Network,” *IET Generation, Transmission & Distribution*, vol. 12, no. 2, pp. 303–309, 2017.

[27] R. Chedid and A. Sawwas, “Optimal placement and sizing of photovoltaics and battery storage in Distribution Networks,” *Energy Storage*, vol. 1, no. 4, 2019.

[28] A. M. Azmy and I. Erlich, “Impact of distributed generation on the stability of electrical power systems,” in Proceedings of the IEEE Power Engineering Society General Meeting, pp. 1056–1063, IEEE, June 2005.

[29] “Innovation for a better life - LG electronics.” [Online]. Available: https://www.lg.com/us/business/download/resources/BT00002151/LGxxxQ1C-A5_350-365W_ck_FRD_V5.pdf.

[30] O. Amanifar, "Optimal distributed generation placement and sizing for loss and THD reduction and voltage profile improvement in distribution systems using Particle Swarm Optimization and sensitivity analysis," 16th Electrical Power Distribution Conference, 2011, pp. 1-7.

[31] A. Konak, D. W. Coit, and A. E. Smith, “Multi-objective optimization using Genetic Algorithms: A tutorial,” *Reliability Engineering & System Safety*, vol. 91, no. 9, pp. 992–1007, 2006.